Gain Stability, Phase Stability And Dynamic Range Measurements Of Analogue Optical Links Used For Radio Astronomy

Roufurd Julie

A dissertation submitted to the Department of Electrical Engineering,
University of Cape Town, in fulfilment of the requirements
for the degree of Master of Science in Engineering.

Cape Town, February 2010

Declaration

I declare that this dissertation is my own, unaided work. It is being submitted for the degree of Master of Science in Engineering in the University of Cape Town. It has not been submitted before for any degree or examination in any other university.

Signature of Author .....

Cape Town

14 February 2010

Abstract

This dissertation investigates the gain and phase stability and dynamic range of an RF-over-fibre optical link as used in a radio telescope. It attempts, via practical experiments, to quantify the gain and phase stability with temperature of the optical fibre and the optical transmitter and receiver. A thermal model based on the KAT-7 environment is then defined and together with the stability coefficients determined, the model is used to qualify the link against the KAT-7 requirements. Measurements of gain and phase stability with temperature (at sunset) and movement of the dish are also performed on the XDM dish (a precursor to the KAT-7) to give an indication of the magnitude of gain and phase change in a real optical fibre link installation. Finally an optical transmitter and receiver set is demonstrated to meet the KAT-7 requirement of dynamic range.

To this end: the KAT-7 requirements for gain and phase stability and dynamic range are motivated and discussed, part of which is apportioned to the optical fibre link; software is developed to to control the VNA (the primary measuring device) and log data and controlled experiments using a thermal chamber and a iButton temperature logger are utilised in the data gathering process.

The results are positive in that an analogue optical fibre link will meet the KAT-7 requirements for gain and phase stability and dynamic range.

In memory of

Fred Fredster

2004–2009

Good times come and good times go. Spaces get occupied. Life goes on

Acknowledgements

I’d like to thank the following people for giving me the support to make this work possible and keeping me honest:

- Mike Inggs, my supervisor.
- The KAT project for their financial support, use of facilities and for all the people there providing guidance and assistance
- My Parents, Wife, In-laws, Friends for their encouragement. Sorry for not giving as much of myself during this time as I ought to.
- God, still keeping it real.

Contents

List of Figures

List of Tables

Nomenclature

Azimuth—Angle in a horizontal plane, relative to a fixed reference, usually north or the longitudinal reference axis of the aircraft or satellite.

Beamwidth—The angular width of a slice through the mainlobe of the radiation pattern of an antenna in the horizontal, vertical or other plane.

DBE—Digital Back end. Contains the digitisers, correlators and data storage of the radio telescope

Doppler frequency—A shift in the radio frequency of the return from a target or other object as a result of the object's radial motion relative to the radar.

DUT—Device under test

NF—Noise Figure

OMT—Orthogonal mode transducer

OTx—Analogue optical transmitter

ORx—Analogue optical receiver

MTBF—Mean time between failure

PRF—Pulse repetition frequency.

RFE—Radio Frequency Front end. The electronics from the output of the OMT of the feed to the point of digitisation in the DBE

Riser cable—The cable which is connected to the fixed (relative to Earth) part of the dish on the one end and the moving part of the dish at the other end. It is used to transfer RF and power signals between the antenna pedestal and the antenna focus. This cable is subject to bending forces and the exposed environment (rain, wind, ambient temperature, sun)

SNR—Signal to Noise ratio

VNA—Vector Network Analyser

Zenith—The antenna dish pointing directly upwards with an elevation angle of 90 degrees.

Chapter 1

Introduction

1.1 Radio Astronomy and Interferometry

Radio astronomy is a sub-field of astronomy that studies celestial objects in the radio frequency portion of the electromagnetic spectrum. The field originated from the discovery that most astronomical objects emit radiation in the radio wavelengths as well as the optical ones.

Some well known single dish radio telescopes include: the Green Bank radio telescope in West Virginia USA, which is the world's largest fully steerable radio telescope with an aperture size of 100 m, the stationary 305 m Arecibo dish in Puerto Rico and the Parkes 64 m telescope in Australia which received the first video transmissions from the moon during the Apollo 11 mission in 1969 [23].

One of the primary goals for radio telescope designers is to increase the sensitivity and spatial resolution of the telescope within practical constraints. One way of achieving this is to build a radio telescope with a bigger aperture (read 'dish'). The widest steerable aperture is around 100 m. Beyond 100 m it becomes impractical to build dishes that will maintain the necessary surface accuracies needed for astronomy [15]. An alternative and more practical way is to synthesise a bigger dish by building multiple smaller dishes and interfering the outputs from the different dishes with each other. This technique of interfering the output of multiple dishes is known as Radio Interferometry.

A well known radio interferometer is the Giant Metre wave Radio Telescope in India which is a Y-shaped array of 14x 45 m dishes with a maximum baseline (largest distance between any 2 dishes in the array) of about 25 km which synthesises a dish with a resolution of 25 km across and the sensitivity of a dish with a diameter of about 250 m.

1.2 The MeerKAT radio interferometer

The Karoo Array Telescope (MeerKAT) project is an initiative by the South African Department of Science and Technology to design and build a radio interferometer consisting

of at least 60 twelve metre dishes by the year 2013. This forms part of South Africa's bid to host the international Square Kilometer Array (SKA) project [22].

The SKA will be a radio interferometer that will have unprecedented sensitivity and resolution in its operating frequency range. South Africa and Australia are short-listed to host the SKA with an announcement due in 2012. More information can be found on the MeerKAT website [www.ska.ac.za].

The KAT-7 radio telescope which is due for commissioning during 2009/2010 is an engineering prototype for risk mitigation and testing. This is an array of 7x 12 m dishes. This phase of the project follows on from the single dish radio telescope phase called the XDM (eXperimental Development Model) situated at HartRAO (Hartebeeshoek Radio Astronomy Observatory).

1.3 Requirement for signal integrity

For radio interferometric imaging to work the radio signals from each antenna need to remain undistorted until the point of being combined. Thus the radio frequency front end receiver chain (RFE) of each antenna–which consist of amplifiers, mixers, filters and the transmission lines transporting the signal–need to ideally:

1. Maintain a constant gain over time
2. Maintain a constant propagation delay over time;
3. Have an infinitely wide dynamic range.

The greater the deviation of RFE from these ideals the lower the quality of the synthesised astronomical images. Radio telescope designers and users of the scientific data have devised calibration techniques to correct for some of the imperfections of the RF instrumentation. Calibration does not correct for all errors however and is only perfect for the instant when it takes place. If there are gain and phase drifts in the parameters after being calibrated, the calibration would be less valid. To minimise the distortions due to these drifts in the parameters, calibration takes place at regular intervals and since it takes a finite amount of time, it decreases the time used to do astronomy.

So the first prize is for the RFE instrumentation to add as little distortion to the information signal as possible. System engineers thus put limits on the imperfections of the components in the RF instrumentation. Or said differently, sub systems of the radio telescope are given specifications which it needs to comply to, so that the radio telescope makes the best astronomical images within a finite budget and finite timescale.

1.4 Optical fibre as a transmission line

Optical fibre is widely used as a transmission line for high data-rate applications and the bulk transfer of digitally encoded information in the field of telecommunications. This is due to its low attenuation per kilometer[1] and practically unlimited bandwidth (> terahertz) properties. It is immune to radiated and conducted interference (RFI), does not conduct lightning, is cheaper than copper for longer transmission paths[2], lightweight and abundantly available (silicon) in nature.

From the radiometer equation, an increase in the amount of bandwidth results in an increase in the sensitivity of the instrument[9]. Due to the increasing demands for sensitivity from radio telescopes optical fibre is increasingly being used in radio interferometry. The configuration shown in Figure 1.1, where digitally encoded data from the individual dishes are transported to the correlator, is commonly used. There are variations of this setup, but this system needs a phase stable clock source (generated by a common clock) at each antenna. The signal received by the antenna is then mixed down and digitised. This time stamped digital data signal modulates a laser light source which transmits the data over an optical fibre to a central correlator station where the various correlation products are formed with the data from the other dishes. Examples of interferometers using this system include the Extended Very Large Array and the Atacama Large Millimeter Array. An advantage of this setup is that the information signal travels a short length (a few ten metres) before it is digitised and since digital data has a higher SNR than analogue data, the integrity of the information signal is assured when it enters the correlator stage some distance away[3]. A disadvantage of this setup is that the digital electronics local to the antenna is a potential source of RFI that can be picked up by the sensitive RF front end.

The optical fibre system illustrated in Figure 1.2 is not as widely used in radio astronomy. Here the suitably band shaped and amplified RF signal, containing the astronomical information, intensity modulates a laser transmitter and the resultant light signal is transported over optical fibre. In the digital back end room some distance away the light signal is detected and converted back to RF, which is mixed down and digitised before being combined with signals from the other dishes in the correlator. A major advantage to Configuration B is that the electrically noisy digital back end is geographically removed from the sensitive dish antenna. A disadvantage is that the RF astronomical signal travels a larger distance than the system in Figure 1.2 and is thus more susceptible to being distorted. Another important disadvantage is that traditionally the optical transmitter used in

[1] Corning LEAF fibre at 1.9 dB/km @ 1550 nm in 2008

[2] In the data communications world, a rule of thumb is that copper is cheaper than fibre up to about 100 m

[3] Provided the CLK signal provided to the mixer at each antenna site is phase stable

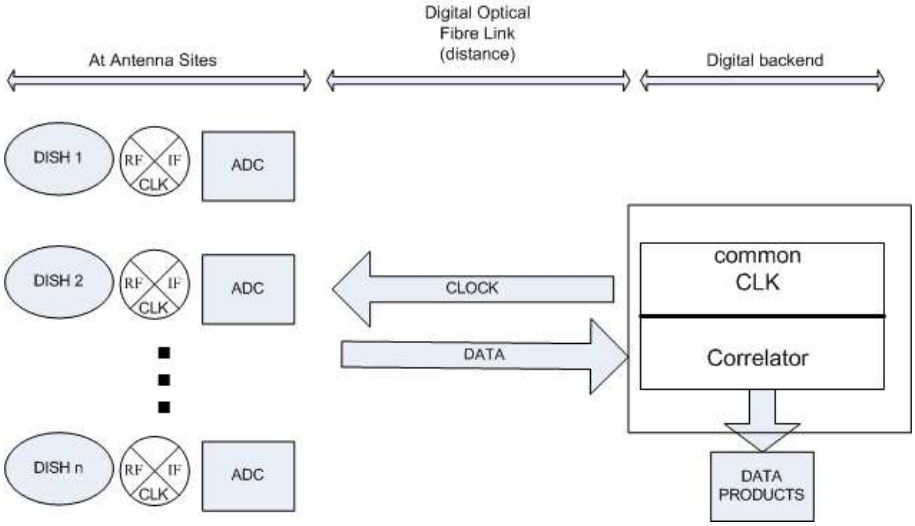

Figure 1.1: Configuration A: A radio interferometer transporting digitised astronomical data over an optical fibre link

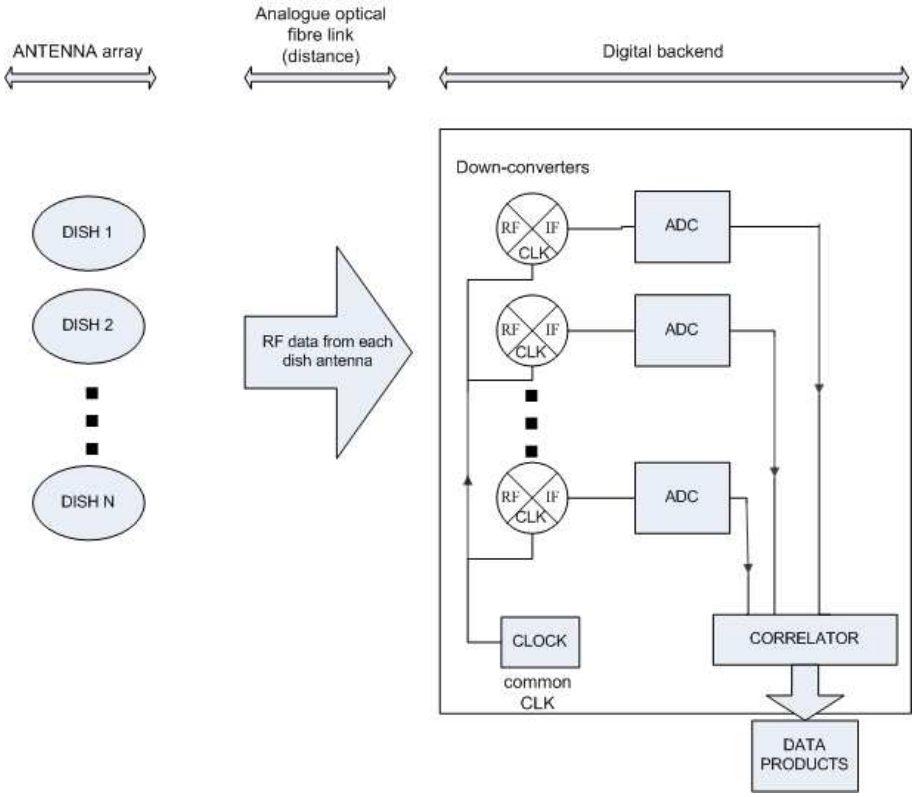

Figure 1.2: Configuration B: A radio interferometer transporting analogue RF astronomical data over an optical fibre

these links have a poor signal dynamic range which has implications for the linearity of the system in a RFI environment. At this time two major interferometers uses this optical fibre installation: the Allan telescope Array (ATA) at Hat creek in the USA, and GMRT in India. Table 1.1 is taken from [10] and summarises the advantages and disadvantages of analogue optical transmission.

Table 1.1: Advantages and disadvantages of analogue optical transmission

Advantages	Disadvantages
Less complex	Very sensitive to parameters affecting RF transmission (Phase, amplitude, temperature, wavelength)
Reduces hardware and bandwidth requirements	System costly and requires less common components
Major hardware located at central location	Requires at least 20 dB SNR at receiver
Reduced risk of radiated interference	Limited dynamic range
No additional skill/training required to build, test and install units	
Easy to maintain	

In both configurations the final outcome is a data product which is further processed to form the astronomical images. The article in [20] gives an introduction to the different ways of transporting astronomical data from a radio telescope over an optical fibre link.

1.5 Optical fibre link in KAT-7

The KAT-7 telescope will make use of a high fidelity, analogue, optical fibre signal transport link. The optical fibre link requirements discussed in this dissertation will be based on the requirements of the KAT-7 dish.

The design of the RF chain in each KAT-7 dish follows the optical fibre configuration in Figure 1.2. The full 1200 MHz to 2000 MHz bandwidth is brought down by coaxial riser cable to the antenna pedestal and then transported using a buried analogue optical fibre link over a 6 km distance.

As mentioned, maintaining the signal integrity of the astronomical signal received by each telescope is important for the image quality of a radio interferometer. Since the radio astronomy community does not have extensive experience in using the optical configuration described in Figure 1.2, the effects on the signal integrity due to this RF front end configuration require careful study. This dissertation attempts to characterise the limitations of an analogue optical fibre link and focuses specifically on gain stability, phase stability and dynamic range properties of the link.

1.6 Objectives

The objectives of this research are to:

1. Understand the gain stability, phase stability and dynamic range requirements of the optical fibre link for KAT-7.
2. Quantify the gain stability, phase stability and dynamic range of an analogue optical fibre link using optical transmitter and receiver units for the KAT-7 receiver chain
3. Develop tools and techniques to measure these performance parameters
4. Conclude on the feasibility of an analogue optical fibre link for KAT-7 telescope

This dissertation thus characterises important performance parameters of an analogue optical fibre link and concludes on its feasibility for KAT-7. The degradation (if any) of performance over time of the key parameters and the reliability of the analogue optical fibre link is not tested in this dissertation[4].

1.7 Plan of development

This dissertation document is structured as follows:

Chapter 1 (this chapter) introduces the topic of radio interferometry and highlights the requirement of signal fidelity of components in the RF chain of the radio telescope front-end. It describes the role of optical fibre link as the means of transporting the astronomical signal in the MeerKAT array and the need to quantify the performance of certain parameters of the link to evaluate its suitability for radio astronomy. The objectives of this dissertation is then stated and the chapter concludes with a description of the development of the thesis.

Chapter 2 introduces the components making up an analogue optical fibre link. It introduces the practice of Calibration in a radio telescope and emphasises that the frequency of the process of calibration is primarily determined by the stability of the radio telescope RF front end. The gain stability, phase stability and dynamic range performance parameters are defined and its relevance to radio astronomy discussed. The requirements from the KAT-7 RF front end are presented and optical fibre link is apportioned a part of the requirement. The apportioned requirements are listed in Table 1.2. The chapter concludes with a thermal model of the KAT-7 environment which will be used to evaluate the optical fibre link against the KAT-7 requirements.

[4] Although if one keeps in mind that the telescope is designed for 20 years and the MTBF of analogue optical transmitters and receivers are of the order of 40 years (Foxcom) and 29 years (Photonics)

Table 1.2: Requirements of the KAT-7 radio frequency front end and the requirement apportioned to the optical fibre link[28]

Performance parameter	RF front end requirement	Apportioned requirement for optical fibre link
Phase stability [max degrees change over 10 minutes or max degrees change due to 10 degrees change in azimuth and elevation movement of the dish]	8	2
Gain stability [max gain change in dB over 10 minutes or max gain change due to 10 degrees change in azimuth and elevation movement of the dish]	0.07	0.03
Dynamic range [dB between noise floor and 1% compression]	40	40

Chapter 3 discusses tools, methods and materials used to measure the performance parameters discussed in Chapter 2. Phase and Gain is measured using a vector network analyser coupled to a computer running the Labview application software. The general setup is shown in Figure 1.3. The uncertainties of the measuring tools are then introduced. The chapter concludes with a description of the optical fibre installation on the XDM dish which is used for some of the experiments.

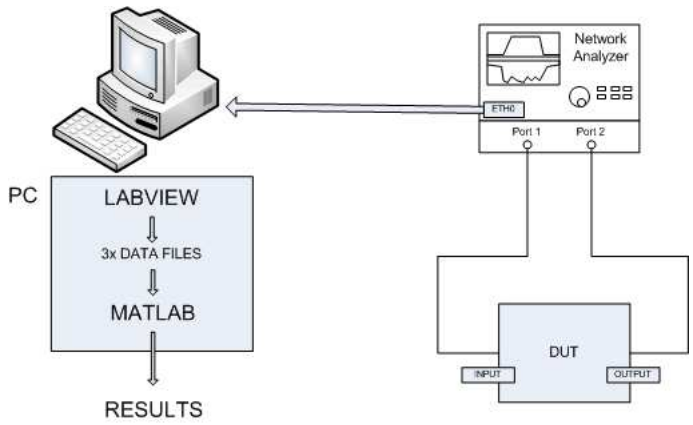

Figure 1.3: General experimental setup to measure gain and phase stability

Chapter 4 describes the experiments and results of gain stability tests done with the Photonics analogue optical fibre link. First the gain stability of a spool of optical fibre was measured. This produced the relationship of 0.00045 dB/km/C $\pm$ 0.00003 dB which showed that for the KAT-7 lengths the optical fibre does not make a significant contribution to the gain stability of the link. Then the gain stability of the optical fibre transmitter and receiver is quantified. This was done by subjecting the optical transmitter and receiver, coupled with a 2 m length of fibre, to temperature changes within a temperature chamber. This produced a result of about -0.02 dB/C as shown in Figure 1.4 and identified the thermal stability of the optical transmitter and receiver as the primary contributor to the gain stability of the link. Using the gain stability figures of the optical fibre and of the

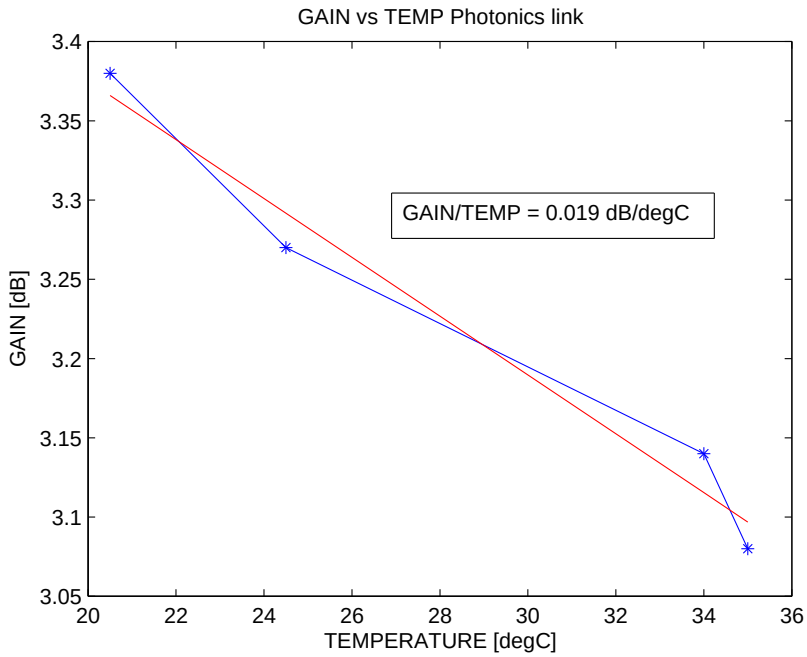

Figure 1.4: Gain change with temperature of Photonics RF-over-fibre transmitter and receiver link (short length of fibre)

OTx-ORx in the KAT-7 thermal model showed that the analogue optical fibre link passes the gain stability requirement of KAT-7. The next experiment was to measure the gain stability of the combined system using a real optical link installed on the XDM telescope. A gain change of -0.00043 dB over 10 minutes during a winter sunset was measured. Finally an experiment was run to check the gain stability performance of the XDM telescope while the dish was being moved. Figure 1.5 shows that the behaviour is repeatable between different runs of the experiment. The worst case change in gain over 10 degrees of azimuth movement is 0.024 dB .

Chapter 5 describes the experiments and results of phase stability tests done with the Photonics analogue optical fibre link. First a fibre spool was placed in a temperature chamber and subjected to temperature changes producing the result in Figure 1.6. This is calculated to be be -20 $\pm$1 degrees/km/C. The phase stability of the optical fibre transmitter and receiver linked by a 2 m fibre patch cord was measured. The change in phase is about 1 degrees with a 15 C change in temperature with an uncertainty of 100%. From this is is concluded that the OTx-ORx does not contribute to the phase stability of the link, especially considering that it is usually placed in a thermally stable environment. These values were then applied to the thermal model of the KAT-7 and it was seen that an analogue optical fibre link passes the KAT-7 requirement. The next experiment was to measure the phase stability of the combined system using an actual optical link installed on the XDM telescope. This resulted in a phase stability of -3.0$\pm$0.3 degrees/C which results in a phase change of about 1 degree over 10 minutes. The phase stability was then checked with movement of the XDM dish. The phase increases by about 2 degrees over 360 degrees of azimuth movement, thus over 10 degrees of movement it makes an

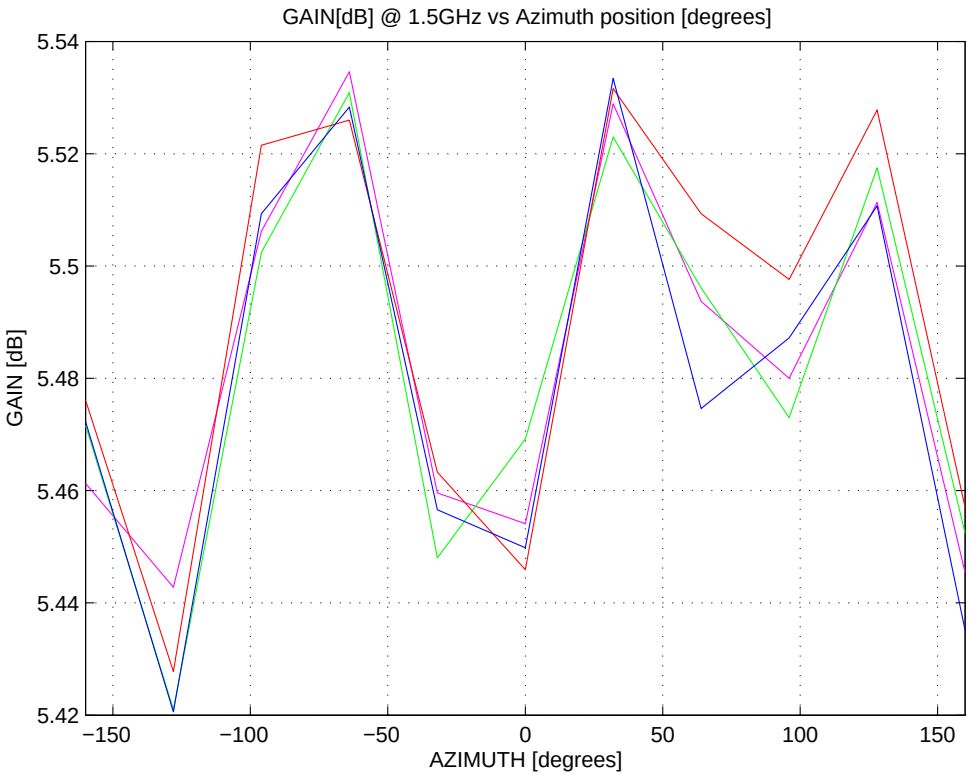

Figure 1.5: Gain changes versus Azimuth position on XDM dish

insignificant contribution to the total phase stability.

Chapter 6 describes the laboratory measurements of the dynamic range of the optical fibre link. A Foxcom link was used as the device under test. A dynamic range of 48 dB was measured and this meets the KAT-7 requirement.

Chapter 7 summarises the results for the gain, phase and dynamic range measurements and compares it to the requirements. It can be concluded that an analogue optical fibre link can fulfill the requirements for the KAT-7 radio telescope. It then concludes this dissertation with comments on the gain, phase and dynamic range results and future work.

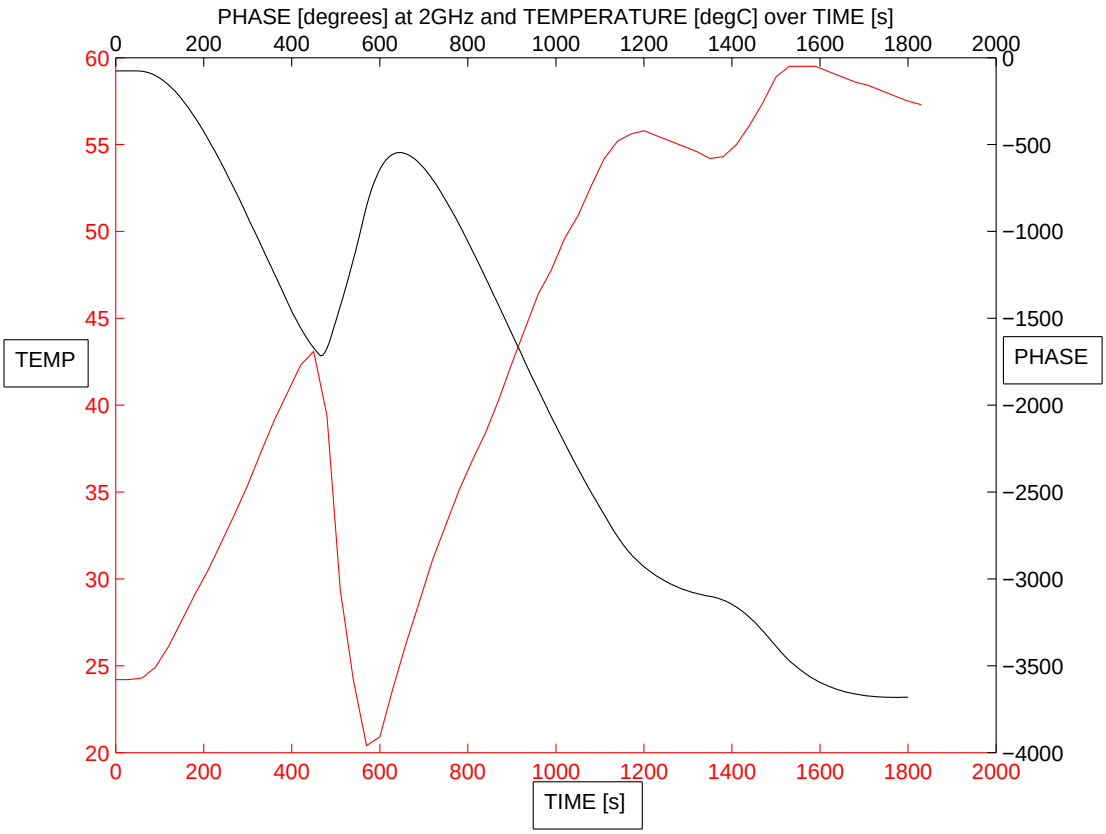

Figure 1.6: Temperature and phase of fibre spool subjected to temperature changes in a thermal chamber

Chapter 2

Analogue Optical Fibre Links, Radio Astronomy Requirements and Definitions

This chapter introduces RF-over-fibre technology. The role of calibration in radio telescopes is explained. The radio interferometer requirements of gain stability, phase stability and dynamic range is defined and the KAT-7 specifications for these parameters are presented. The chapter concludes with a synthesis of a thermal model which is based on the KAT-7 thermal environment and against which the analogue optical link will be tested

2.1 What is an analogue optical fibre link?

An optical fibre link is a system consisting of: an optical laser transmitter, a light guiding medium and an optical detector. In this dissertation it is defined as a system that takes as input a RF signal which intensity modulates the optical laser light of the transmitter. The light output is transported over some distance to the other end of the link via the optical fibre, which is normally protected within a cable. The RF signal is recovered by a light detector inside the optical receiver. This system is illustrated in Figure 2.1.

2.1.1 The Optical transmitter

Optical light sources for optical fibre can be divided into 2 categories: monochromatic incoherent sources (LEDs) and monochromatic coherent sources (lasers). For reasons explained in [25], the laser diode is the most commonly used light source for high fidelity communications over single mode fibre. Some of the factors include its narrow spectral bandwidth, its size and configuration being compatible with launching light into an optical fibre and that it couples sufficient power into the optical fibre to overcome the transmission losses.

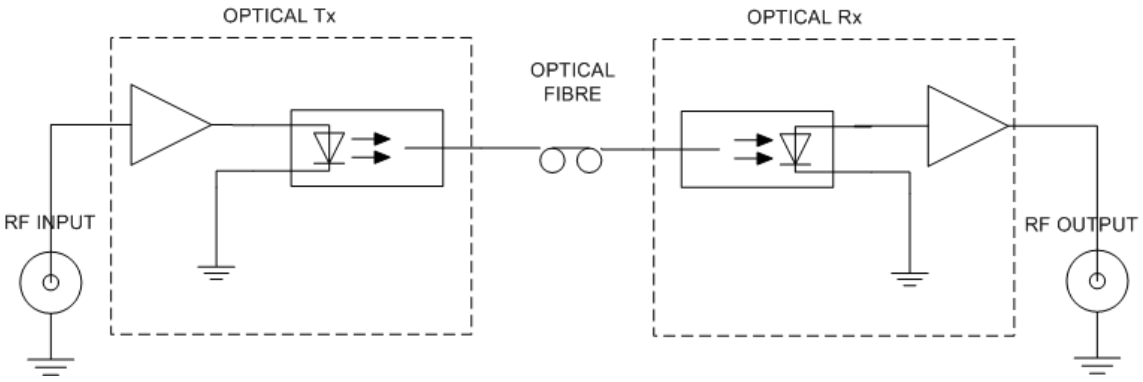

Figure 2.1: Optical fibre link block diagram

The optical transmitter component, used for analogue transmission, usually consist of the laser diode and the lasing cavity which emits at a specific wavelength. At the current state of technology, intensity modulation is the most widespread means of modulating the laser light travelling over the optical fibre. Intensity modulation is realised by either controlling the power output of the lasing mechanism, which is known as direct modulation, or having a fixed lasing system and having a component to modulate the emitted light and is classified as indirect modulation (for e.g. Mach Zehnder modulators). [5] provides an introduction to the different kinds of modulation.

2.1.2 The Optical fibre transmission path

Optical fibres are waveguides for the light waves emitted by the optical transmitter. As a waveguide, it has low loss[1], is a dispersive medium and is linear at the power levels that the analogue optical transmitter used in this dissertation emits at (< 10 mW). An optical fibre consists of a core and a cladding as shown on the right hand side of Figure 2.2. The size of the core determines how many modes of the electromagnetic wave (the light wave) propagate. This separates optical fibre into 2 broad classes: single-mode and multimode (see Figure 2.2). Multimode fibres have core diameters of 50 μm and more, allowing many modes of the electromagnetic wave to propagate. Single mode fibre has a typical core size of 9 μm and allows only 1 mode to propagate. For analogue signal transmission in radio interferometry, where signal integrity and the maintenance of phase information is important, single mode fibre is used.

2.1.3 The Optical receiver

At the receiver end of the optical fibre transmission line the optical information is detected in an optical receiver. As explained in [5], to recover an intensity modulated optical carrier requires: 1) a material that can absorb the optical wave, 2) A device structure that can be fabricated in this material and 3) the ability to collect the carriers generated by the

[1]Corning LEAF fibre optical attenuation at 0.19 dB/km @ 1550 nm in 2008

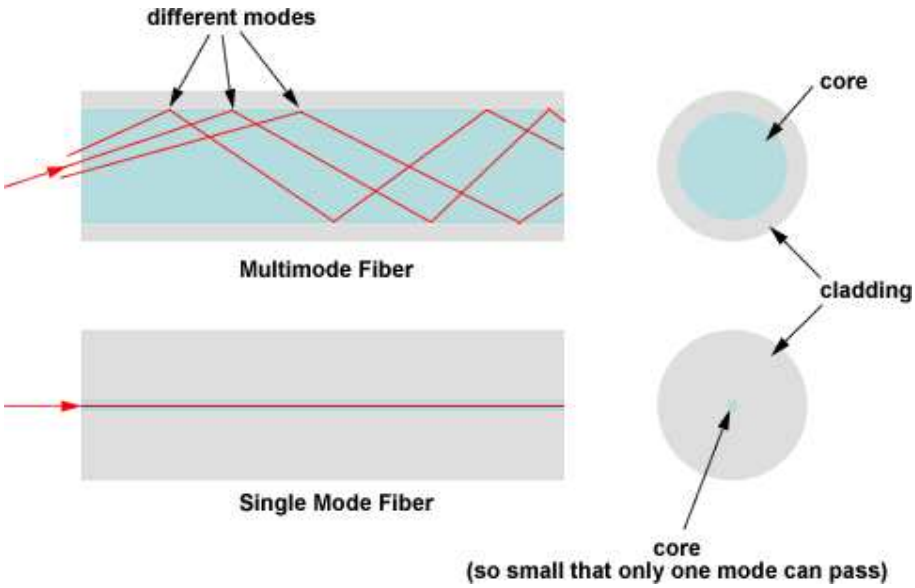

Figure 2.2: Multimode and single mode optical fibre. The core of single mode fibre is about 5 times that of multimode fibre allowing only a single mode of the electromagnetic wave to propagate.

absorption and to convey them to an external electrical circuit. The external circuit consist of a trans-impedance amplifier and further amplification to bring the recovered RF signal up to a usable level.

2.2 Calibration

Before discussing the performance requirements of the optical fibre link it is important to introduce the process of calibration of a radio telescope. Calibration, as used in radio astronomy, is the process of correcting the astronomical data for measurement errors due to the radio telescope's instrumentation[2]. The calibration parameters of interest in this dissertation include gain and phase stability errors. A list of stable extraterrestrial sources is periodically published with accurately measured power spectra (or flux density). A radio telescope regularly points to these sources (if visible at the time) and compare what is measured with what is expected (as contained in this list) . This generates an error data set which is then used to correct the subsequent set of astronomical data received with the telescope in that calibration cycle.

Calibration of a telescope takes up scientific time during the operation of the telescope and thus its frequency needs to be minimised. The gain and phase stability are primary determinants of how often the calibration process is performed. Better stability of the receiver instrumentation means longer periods between calibration and consequently a more efficient astronomy instrument. A time often mentioned is the scan time, which is the time that observations take place between calibrations. In KAT-7 a scan time of at

[2]Calibration also corrects for errors due to the earth's changing atmosphere

least 10 minutes is sought[11]. These requirements are based on planned astronomical functions of the telescope.

2.3 Performance definitions and requirements for KAT-7

As mentioned, radio astronomy places stringent performance requirements on the RFE (radio frequency front end). The following performance parameters of the optical fibre link are critical to the performance of the radio interferometers when used in the receiver chain:

1. Gain stability
2. Phase stability
3. Signal level dynamic range

Each of these requirements will now be defined in this chapter and its relevance to radio astronomy discussed.

2.3.1 Gain stability requirements

Gain stability can be defined as the drift in the gain (or loss) of a component over time.

The equivalent input system noise temperature T_s of the KAT-7 RFE is expected to be of the order of 20 K. The astronomical signal is buried in this noise. Since the nominal output power level which is passed to the digitiser is P_o = -30 dBm in a bandwidth of 800 MHz, a net gain of $kT_sB/P_o = 70$ dB is required. With various cable, splitter and other losses in the system the actual gain may be somewhat higher. When considering design goals like minimising the system noise temperature and maximising the dynamic range of the system, this gain will be distributed throughout the RFE chain (This paragraph is adapted from [6]).

To support total power radiometry it is required that the net gain be stable between calibrations. Gain stability also has an influence on the sensitivity of the radio telescope. The gain stability requirement for the RFE of KAT-7 is as follows:

Gain stability of the whole RFE : 0.07 dB change over 10 minutes and less than 10 degrees of movement in azimuth or elevation

Since there are multiple components forming part of the RFE chain this requirement needs to be apportioned between each component. The optical fibre link has thus been apportioned the following requirement:

Gain stability of optical link : 0.03 dB over 10 minutes.

2.3.2 Factors that influence the gain stability of an analogue optical fibre link

Change in temperature of the laser transmitter and receiver

The average output power of the laser link decreases/increases when its temperature increases/decreases. Measurements done on the Miteq link (with 1 metre of fibre) showed a linear drift in the gain @ 1.5 GHz of -0.03 dB/C. This requires that the optical transmitter and receiver be temperature stabilised. The Foxcom unit to be used in KAT-7 has a factory measured gain stability of ± 0.004 dB/C. Since the Foxcom unit will be thermally coupled to a 25 ± 1 C water cooled plate, ± 0.008 dB is the expected stability. Section 4.2 describes the experiment and results to measure the gain stability of the Photonics optical transmitter and receiver.

Bending of the optical fibre

The Corning LEAF datasheet [4] states a change in attenuation of < 0.5dB/km for a bend of 1 turn around a 32 mm mandrel. This will not have an effect for the KAT-7 telescope since the optical fibre cable will buried and not subject to movement during operation. It is an issue for a Configuration B (see Figure 1.2) radio telescope if an optical fibre riser cable is used. The riser cable is the cable between the pedestal and the antenna focus and is thus subject to bending and torsion where it passes through the azimuth and elevation cable wraps. A technical explanation for the losses due to bending is explained in section 3.6 of [25]. Basically, for a particular wavefront, the part of the wavefront on the outer radius of the bended fibre waveguide need to travel faster than the part of the wavefront on the inner radius. Since it cannot do so, some of the energy escapes into cladding causing a loss[3]. Section 4.5 describes the experiments and results of gain measurements made on the XDM optical link during movement. Appendix B describes the mechanism of the XDM cable wraps

Change in temperature of the optical fibre

The Corning LEAF fibre datasheets states a worst case light attenuation of 0.05 dB @ 1550 laser wavelength, with a change in temperature of -60 C to +85 C. This is less than 0.0014 dB/C/km for the RF signal assuming that the gain (or loss) is linear over temperature. Section 4.1 describes experiments and result of the gain stability of an optical fibre spool subjected to temperature changes.

[3] An other effect on the amplitude of the wave during bending/torsion of the optical cable is the changing polarisation mode distortion (PMD). This would manifest more as an additional noise on the output signal and less as an average gain change affecting the gain stability that we're interested in in this dissertation. The effect would also be small for the < 5 GHz RF signals being considered in this dissertation.

Aging[4]

Silicon fibre has a water peak in the 1360 - 1460 nm spectral band. This results in absorption of light energy of this wavelength travelling in the fibre and thus an attenuation in the optical link. Optical fibre manufacturers have managed to reduce this water peak in modern fibres. Over time however water molecules get reabsorbed into the fibre and this results in increased attenuation of the optical link. This aging effect can however be assumed to happen on durations >> 10 minutes and is thus removed by calibration.

Power supply stability

A figure of 0.06 dB/V gain stability for supply variations has been quoted[5] for the Foxcom optical link. Power supply stability thus needs to be considered during the design of the power supply for the optical transmitter and receiver. It is not measured in this dissertation

2.3.3 Phase stability

Phase stability can be defined as a drift in the phase at a specific frequency component in the transported signal over time. The phase Θ of the transmitted signal is directly proportional to the propagation delay τ and is given by:

$\Theta = 2\Pi f_0 \tau$ in radians

$\tau = \frac{\Theta}{2\Pi f_0}$ in seconds

Where f_0 is one of the frequency components in the transmitted signal.

The propagation delay (and thus the phase) of a signal travelling through the optical fibre varies with fibre thermal expansion and change in fibre refractive index with temperature and tension[3].

In radio interferometry phase stability is a critical requirement for the telescope. The greater the phase instability, the greater the level of decorrelation of the synthesised beam. Decorrelation causes a decrease in sensitivity and resolution of a radio interferometer.

Note that decorrelation happens due to phase differentials (after calibration) between the signal paths of the many antenna-receiver systems making up the the interferometer. Thus if on each path the total phase change is equal, then the interferometer as a whole is still operating at ideal performance in terms of phase stability. The differential phase stability requirement for the RFE is:

Phase stability of whole RFE : 8 degrees RMS @ 2 GHz over 10 minutes and less than 10 degrees of movement in azimuth or elevation

[4]The information in this paragraph was explained during private communications with an optical fibre engineer, Dirk Wolmarans of CBI-Electric in South Africa during 2009

[5]This was during private discussions with Foxcom and is not a figure normally quoted in their datasheets

The phase stability requirement apportioned to the RF-over-fibre link is:

Phase stability of optical link : 2 degrees RMS @ 2 GHz over 10 minutes

2.3.4 Factors that influence phase stability of an analogue optical fibre link

Change in temperature of laser transmitter and receiver

The greater the group delay of an active component the more susceptible this component is to phase instability. This is true because group delay over a band is the derivative of the phase change. Thus equal positive % changes in group delay with temperature will cause a bigger change in phase in the higher group delay device than the lower group delay one. The optical links worked with in this dissertation have group delay specifications of the order of 10 s of ns. Group delays in the Miteq, Photonics and Foxcom devices are 10 ns, 62 ns and 20 ns respectively. In Section 5.2 an experiment measuring phase change with temperature of the OTx-ORx is performed and the Photonics device's had a phase change of about 1 degree over a 15 C change in temperature. With the optical transmitter and receiver being in a relatively stable temperature environment its expected to have an insignificant effect on the phase stability of the link.

Bending of optical fibre

The bending of the optical fibre causes tensile stresses and thus the refractive index of the fibre to change at areas local to the bend[3]. Refractive index changes cause changes in the propogation delay of the light down the fibre and thus the phase to change. Experiments measuring phase stability due to movement on the XDM link are described in Section 5.5 and showed insignificant effects due to bending.

Change in temperature of optical fibre

As will be seen, temperature is by far the most significant contributor to phase instability in the optical link. Temperature changes on the fibre cause the refractive index to change, which causes the propogation speed and thus the propogation delay to change [3]. Changes in temperature of the fibre also result in thermal expansion/contraction which increases/decreases the propogation delay (thus phase) of the signal down the fibre[6]. A value listed in [7] for delay stability of non-cable optical fibre is -8 ppm/C . In KAT-7, most of the fibre will be buried at least 1 metre deep and thus phase stability is expected to be sufficient over 10 minutes (see Section 2.4.2 later). In the MeerKAT dish where an optical fibre riser cable will most likely be used (due to the greater bandwidth requirements),

[6]This is not as big a problem as the refractive index changes at the < 5 GHz frequencies of KAT-7

phase stability need to be optimised with the design and routing of the cable. Sections 5.1 and 5.4 describe experiments of phase stability with temperature changes on the fibre.

Aging

No information have been found in literature[7], but any effects are likely to happen over timescales much greater than 10 minutes.

2.3.5 Dynamic range

Signal level dynamic range of the receiver of a component used in the RF chain is defined in this dissertation as the ratio between the 1% gain compression point and 20 dB above the noise floor. The primary requirement for dynamic range in radio astronomy is to do quality radio science in the presence of RFI.

Desired SNR as the lower level

As stated above dynamic range is determined by 2 levels. The lower level is determined by the desired SNR (signal to noise ratio) by components after the LNA. SNR is a common parameter used in the design of RF receiver systems in telecommunications. A 20 dB SNR at the input of a component means that the noise contributed by that component in the chain is 1/100th of the information signal level. SNR is thus a function of the noise floor of a component and the nominal signal at the input of the component.

The upper level due to gain compression and RFI distortion

The upper level exists due to the normal occurrence of saturation in a linear and active RF component at the higher input powers where the gain transfer function becomes non-linear. The 1dB gain compression point is defined as the input power level where the output signal is 1 dB down from the theoretical power level if compression did not occur. Figure 2.3 illustrates the input and output gain compression points.

Due to the increasing non-linearity as the input signal approaches the saturation level of the amplifier, mixing of the input frequency components occur. Of particular concern are the 3rd order inter-modulation products as these are potentially within the operating band. The 3rd order inter-modulation products are represented by $2f_1 - f_2$ and $2f_2 - f_1$, where f_1 and f_2 are in-band frequencies. Thus if $f_1 = 1.5$ GHz and $f_2 = 1.4$ GHz, then $2f_1 - f_2$ and $2f_2 - f_1$ equals 1.6 GHz and 1.3 GHz respectively. All amplifiers generate these 3rd order products. The lower the level of input signal to the amplifier relative to its 1dB compression point the lower the level of the inter-modulation products.

[7] There have been papers describing permanent changes in length of fibre which could affect the absolute phase shift as it passes through the system, but this happens over extreme temperature excursions and would not be applicable for the conditions in radio astronomy. Unless of course a radio telescope is build in space!

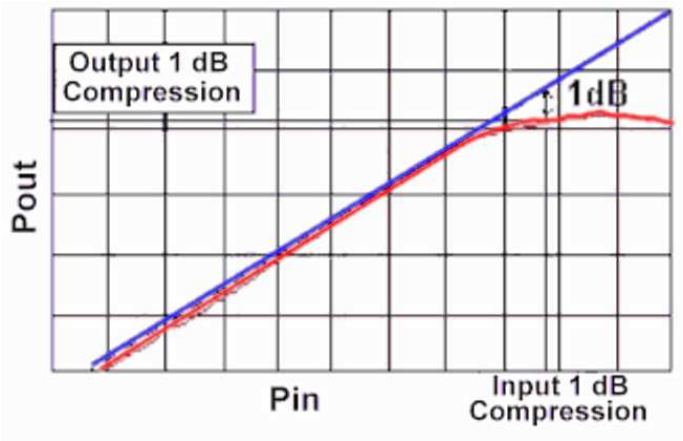

Figure 2.3: Plot illustrating 1dB gain compression (taken from www.spectrummicrowave.com). The red graph illustrates the real transfer function and the blue graph represents the ideal system where saturation does not occur.

Even in the relatively radio quiet environment of the Karoo, the KAT-7 telescope will still be subjected to radio interference. A particular problem is the GPS and Afrisat set of satellites and distance measuring equipment (DME) signals from passing aircraft. These signals operate inside the KAT-7 operating band and are much stronger than the radio astronomy sources the radio telescope is observing. Even when not pointing the telescope directly to these satellites interference can still be picked up via the antenna sidebands. In the KAT-7 system the entire band is transported (thus no notch filtering) through the RF chain and then digitally channelised. If any of the frequency channels are affected by RFI they are discared. This works provided the dynamic range of the RF chain is sufficient, as when the amplifier saturates, information from all the frequency channels in the band are corrupted.

To minimise the inter-modulation distortion the receiver should be designed to behave linearly even in the presence of the relatively powerful man-made interference. Radio telescope designers thus use the 1% compression point as the upper level for the devices in the chain. It has been shown in [18] that the 1 % compression point is 14 dB below the 1 dB compression point. At 1 % compression the fundamental (information) signal is down 2 % while the inter-modulation products are down by an acceptable 48 dB.

Dynamic range requirement for the optical fibre link

The desired SNR and the 1% compression thus define the dynamic range requirement for each component in the chain (for components after the first LNA). The designer of the RFE chain should choose the components and design the gain distribution such as to get the desired dynamic range and SNR throughout the system. For KAT-7 the optical fibre link requirement is as follows:

RFE Dynamic range requirement : With a SNR of 20 dB the headroom to 1% compression $\geq$ 20 dB.

2.4 Definition of thermal environment in which the optical fibre link will be qualified

As seen earlier, temperature changes are the primary contributor to the gain and phase stability of the optical fibre link. To determine whether the optical fibre link will meet the gain and phase stability requirements, the thermal environment of the link needs to be defined. The requirements defined in this section are related to the KAT-7 environment. The optical fibre link is distributed over 4 environments: 1) the antenna pedestal where the optical transmitter is located, 2) the 5 km underground section where the optical fibre cable is situated, 3) transitional cable between the underground fibre cable and the patch panels, and 4) the computing container where the optical receiver is situated.

2.4.1 Thermal environment of the optical transmitter at the antenna pedestal

For KAT-7 the optical transmitter is mounted on a temperature controlled platform. The platform consist of a hot and a cold plate with peltier coolers in the center. Temperature control of the cold plate is done via PID controller and the cold side of a peltier cooler. Excess heat on the hot side of the peltier is removed with an aluminium plate with 25 C $\pm$ 1 water circulating through it. The cold plate is controlled to within 0.05 C of a setpoint. Temperature changes and thus temperature stability over 10 minutes would thus be negligible.

A cost and reliability saving can be made by removing the peltier circuitry altogether. This leaves the optical transmitter to be subject to the $\pm$1 C water cooling for KAT-7. The optical transmitter gain stability contribution will be estimated on the assumption that its platform changes by $\triangle$2 C worst case over 10 minutes[8].

2.4.2 Thermal environment of the underground optical fibre cable

In KAT-7 the underground portion of the optical fibre cable is buried at least 1.2 m underground[9]. For the 5 km stretch of buried optical cable inside a duct with an effective depth of about 1.2 m an estimate of the variation in temperature experienced by the buried

[8]This requirement is not based on any previous experience and created for purposes of having a definition. Under steady state and normal operation the KAT-7 electronics would not generate enough energy to heat the water by 1 C within 10 minutes. From practical experience of the water coolers installed in the Karoo, there is an immeasurable change in the water temperature over 10 minutes. The tolerance on the water specification is entirely due to the unlikely situation of > worst case heat loads on the water cooling lines.

[9]It is in fact placed inside a sub duct and not directly buried. For the analysis in this section it will be assumed that there is no air flow inside the duct and that the thermal environment inside the duct is the same as if the cable was buried directly in the soil. This is a fair assumption as the KAT-7 ducts are specified to be sealed for air flow at both ends. Air flow through the duct would negate the thermal insulation provided by depth of burial of the cable

cable is expressed as: $dT = dT_{env}e^{(-d/D)}$ where dT_{env} is the environmental variation, d is the depth to which the cable is buried and D is the scale depth of the soil, expressed as $D = \sqrt{\frac{\eta P}{\pi}}$ where η is the soil's thermal diffusivity and P the period over which the temperature change takes place[27]. With an ambient temperature change of 15 C to 45 C over 24 hours[10] giving a dT_{env} of 30 C and with the soil's thermal diffusivity at around 0.18 [$\times 10^{-6} m^2 s^{-1}$] (for the dry clay soil in Carnarvon[11])[12], the temperature variation at a depth of 1.2 m would be 1×10^{-6} C over a period of 24 hours. This is practically 0 C temperature change in the thermal environment of the optical fibre cable. This component to the thermal model will thus be ignored.

2.4.3 Underground to Receiver rack / Pedestal transitional fibre cable

When considering the optical fibre cable at the exit and entrance points to the underground cable let's for the worst case assume that 10 m of cable (5 m on each side of cable) is exposed as it gets connected to the optical transmitter and receiver. These cable lengths will be in the shade and for the worst case, let's assume that the cable will follow a cycle of 10 - 30 C over a period of 24 hours. This equates to a max change in temperature of 0.28 C in 10 minutes.

2.4.4 Thermal environment of the optical receiver at the digital back end container

This environment is equivalent to the transmitter environment of $\triangle 2$ C over 10 minutes.

2.5 Summary

The 3 components constituting the optical fibre link have been identified. The calibration process has been introduced, its relation to phase and gain stability explained and some of its shortcomings have been mentioned. The SCAN time has been defined and is the time in which gain and phase stability requirements are defined. The 3 important RF performance requirements of gain stability, phase stability and dynamic range, have been defined and its relevance to radio astronomy discussed. Some of factors affecting the gain and phase stability have been identified and explained. An environment based on KAT-7 is defined in which the gain and phase stability of the analogue optical fibre link will be tested against the KAT-7 requirement.

[10] typical hot Summer day at the KAT-7 site

[11] This thermal diffusivity value can be found at many sources, I found it @ http://apollo.lsc.vsc.edu/classes/met455/notes/section6/2.html during January 2010.

[12] If the soil is moist this value is smaller, i.e. heat flows through quicker thus decreasing the thermal insulation properties

Chapter 3

Tools, Method and Materials

This chapter discusses the methods and materials used to perform the experiments contained in this dissertation. A set of tools are described which measure the gain and phase of a generic device under test and outputs this information to text files. It summarises the main features of the optical terminal devices used as the source and detector to measure the properties of the optical fibre. A section on measuring certainty is presented. Finally the XDM fibre installation at HartRAO is described, which is used to generate the dataset for some of the results of this dissertation.

3.1 Starting with the measuring tools

3.1.1 VNA

The Rhode & Schwarz ZVB8 vector network analyser (VNA) was available for the duration of the experiments described in this dissertation. A VNA measures the scattering parameters of a network over a user-defined frequency range. Scattering parameters are explained in [14].

For the purposes of this dissertation the S21 parameter is required in this 2 port system as it represents the transmission coefficient of the DUT. The required phase and power gain data is calculated internally by the VNA using the raw S21 data.

Before the VNA can be used to measure it is required to be calibrated. Calibration removes the effects[1] of the test cable lengths which connect the device under test (DUT) to the VNA and other effects internally to the VNA. The R&S ZV-Z51 automatic calibration kit was available to calibrate the ZVB8.

The VNA has an ethernet port which allows a user PC, via the local area network (LAN) and using the defined protocol, to control the functions of the VNA and download data from it. This allows a software application program, like Labview which is installed on

[1]These are the static effects. It cannot do anything about post-calibration bending and temperature changes of these cables

user PC, to control the VNA and download the measured data from it. All these features are covered in the ZVB user manual [26].

3.1.2 Noise Figure Meter

NF is a ratio defined as $NF = \frac{SNR_{out}}{SNR_{in}}$, where the input is a matched load at 293 K. Thus it is a measure of the additional noise contributed by a DUT at the output when the input to the DUT is terminated in a matched load at 293 K. This information can be used to determine the absolute noise power contributed by the DUT inside a given bandwidth. NF can be measured using a hot and cold load connected to the DUT and using the outputs of the DUT together with Y-factor method to calculate noise figure of the DUT as explained in [19].

A NF meter measures the NF using the Y-factor method. It uses a noise head as the input load which contains a noise diode producing a calibrated noise output. When the noise diode is on it produces a noise temperature which is multiple times the room temperature and this is regarded as the hot load. When it is off it produces a matched load at room temperature and this noise level is considered the cold load. The ratio between the hot and cold output levels coming out of the noise head is called the Excess Noise Ratio (ENR)[1].

Measurements of NF for the results in this dissertation was done with an Agilent N8975A using a noise head with ENR of 6 dB. Before the NF meter can be used to measure NF it needs to be calibrated. This measures the noise head's hot and cold temperatures during that specific measuring session and this goes into the Y factor calculation.

3.1.3 Labview

"Labview (short for **Lab**oratory **V**irtual **I**nstrumentation **E**ngineering **W**orkbench) is a platform and development environment for a visual programming language from National Instruments... Labview is commonly used for data acquisition, instrument control and industrial automation on a variety of platforms including Microsoft Windows, various flavors of UNIX, Linux, and Mac OS...." (taken directly from [29]).

After installing the PC drivers which provides the API (application programming interface) to enable the VNA to be accessed over the ethernet, Labview code was developed in accordance with the controlling protocol described in [21]. This program collects VNA data at a user settable number of 1 minute intervals. The user interface is shown in Figure 3.1.

The Labview software expects 3 channels to already have been setup on the VNA before it is executed. The output of the Labview program are 3 text files representing the gain, group delay and phase data. The full details of the Labview program can be found in Appendix A.1. Matlab was used to extract, analyse and plot the information from these data files.

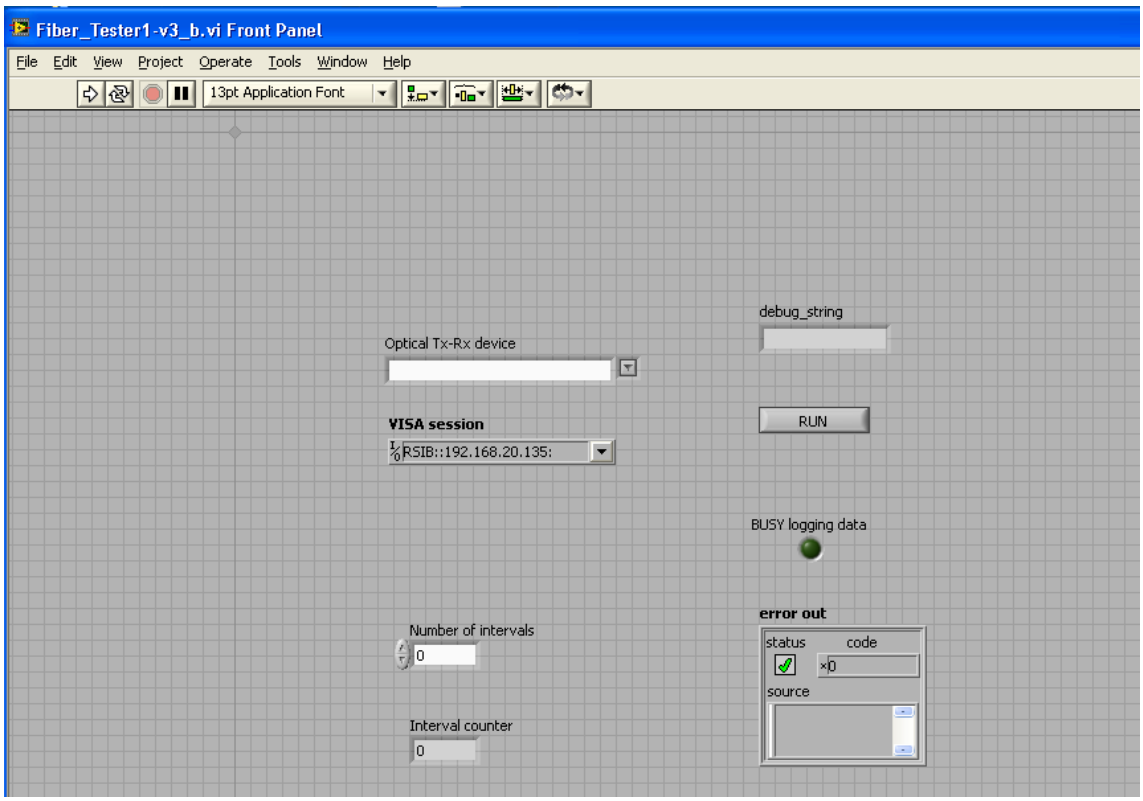

Figure 3.1: User interface to Labview program controlling the VNA

3.1.4 Matlab

"MATLAB is a numerical computing environment and programming language. Created by The MathWorks, MATLAB allows easy matrix manipulation, plotting of functions and data, implementation of algorithms, creation of user interfaces and interfacing with programs in other programming languages" (taken directly from [30]).

Matlab was used to extract data from the text file, format the data, do signal analysis and plot the data inside the files created by Labview program described above. Standard Matlab commands were used to do the data analysis.

3.1.5 Measuring temperature

Two tools were used to measure temperature: 1) The FLUKE multimeter with attached thermocouple; 2) the iButton temperature logger.

FLUKE multimeter

The Fluke 189 multimeter has a mode which allows temperature to be measured with a thermocouple and logged at a user settable sampling rate. The actual sensor is the pin size head of a thermocouple which attaches via a 1 metre cable to the multimeter. The data is downloaded from the multimeter using the Flukeview Forms PC software.

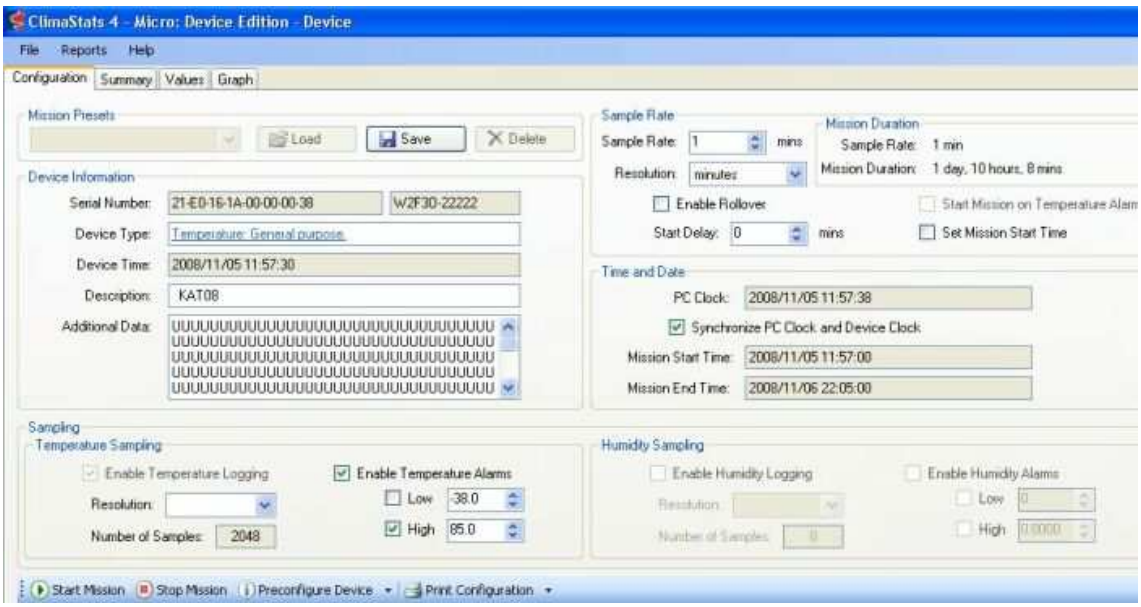

Figure 3.2: Screenshot of iButton configuration in Climastats software

iButton temperature logger[2]

The iButton is a temperature sensor, data logger, real time clock, with internal battery sitting inside a 5 mm high, 10 mm wide cylindrical, ruggedised, metal container. It has a user settable sampling rate from 1 minute to 4 hours, and can store from 4000 date-time stamped temperature readings with a temperature resolution of 0.5 C. Data is downloaded to a PC using a button reader, which is a suitably shaped USB to 1-wire interface with the appropriate application PC software.

The PC software is Climastats version 4 and is a commercial product of Fairbridge Technologies (http://www.fairbridge.co.za/). A screenshot of the configuration screen is shown in Figure 3.2

3.1.6 Overview of measuring tools

An overview of the measuring tools is illustrated in Figure 3.3.

3.2 The optical link as the DUT

The analogue optical fibre link consist of 3 components: the laser transmitter with integrated laser modulator, the optical fibre signal transmission line and the light detector. From a system point of view, it consist of an RF input and a RF output. These ideas are illustrated in Figure 2.1. The Photonics 1602 link was available to test the optical fibre. The Foxcom 7310 is the other link used in this dissertation for the dynamic range measurements.

[2]More information can be found at http://www.maxim-ic.com/products/ibutton/ibuttons (accessed on 05/11/2008)

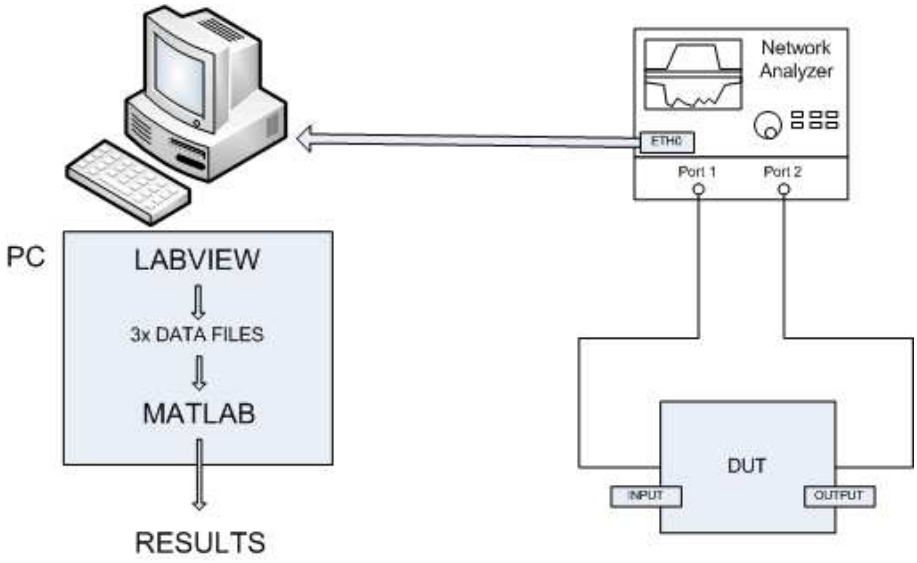

Figure 3.3: Overall diagram of measurement setup

3.3 Measuring uncertainty

This section does an analysis on the uncertainty in the results which will be described in later chapters of this dissertation and proposes an error bar within which measurements can not be measured precisely. Here will be reported on an experiment done on the VNA with its test cables to determine the uncertainty of the measuring system.

3.3.1 VNA and test cable stability and uncertainty[3]

All experimental measurements were done in air conditioned laboratories using the VNA and test leads. The following analysis is thus applicable to all the results. The ambient temperatures surrounding the experiment are controlled to ± 1 C by air conditioning. The VNA, as with most RF systems containing amplifiers and mixers etc, has its own gain and phase stability performance with temperature. Another factor is the uncertainty in the detector of the VNA where one contributor would be the quantisation error of the analogue to digital converter inside the VNA. The VNA specification sheet lists the following specifications:

Gain stability = 0.05 dB / K

Gain Uncertainty = 0.03 dB

Phase stability = 0.4 degrees/K

Phase Uncertainty = 0.2 degrees

The test cables used also has a temperature dependent performance. Data found in [7] for the RG223/U cable used indicate that it has a phase coefficient of -70 ppm/C in the

[3]Note that in the analysis in this section changes in the measuring accuracy with temperature is not considered. It is assumed that the accuracy is constant over the ambient temperature ranges that the VNA is subject to and thus cancels out when calculating the $\triangle$parameters which are needed.

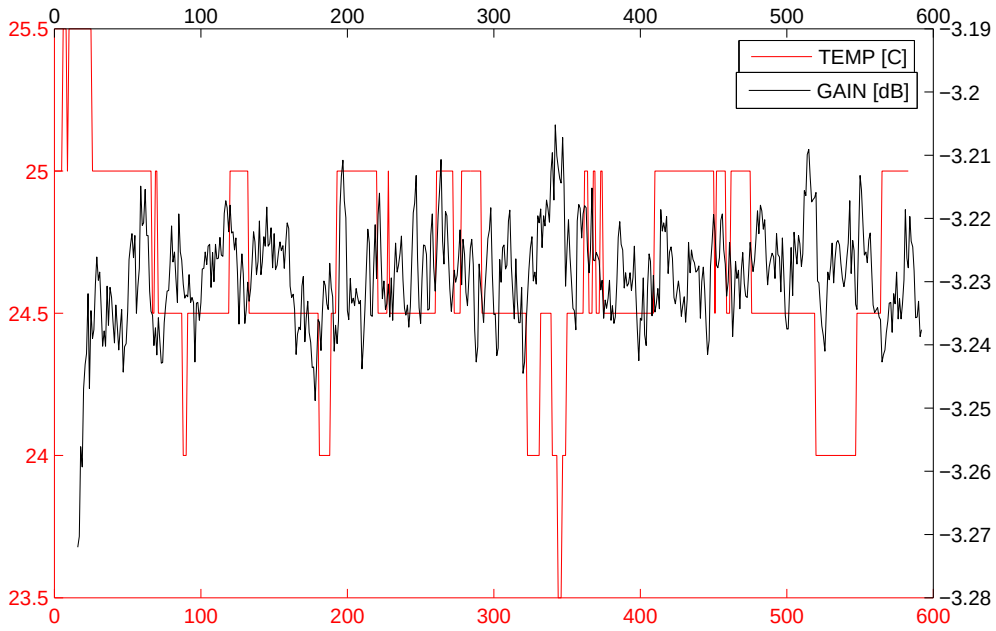

Figure 3.4: Demonstration of VNA gain stability with temperature changes over 4 days

room temperature range. The gain change is assumed to be negligible for this length of cable. The total uncertainty can thus be seen as the sum of the individual uncertainties as captured in the following equation:

Gain stability = VNA contribution + Test lead contribution = $(0.05 \times 2 + 0.03)$+(small) $= 0.13$ dB

Phase stability = VNA contribution + Test lead contribution = $(0.4 \times 2 + 0.2) + (1) = 2$ degrees

3.3.2 Putting the measuring uncertainty into perspective

An experiment was run over 2 days in the laboratory using the setup described in Figure 3.3 with the DUT being a 3 dB attenuator tightly wrapped in styrofoam. The styrofoam was used to isolate the DUT from ambient changes. Any temperature dependence of the attenuator value can thus be ignored thereby leaving the VNA-test cable system as the only variable. An iButton sensor was used to measure the ambient temperature in the locale of the VNA.

Figure 3.4 show the temperature and measured gain variation of the VNA-test cable system over 4 days. The first thing we notice is the roughness of the plot. This is an indication of the 0.03 dB VNA uncertainty mentioned earlier. Over time we see a negative correlation with temperature. There is a peak change of about 0.1 dB with a peak change in temperature of 2 C. This roughly agrees with the worst case change of 0.13 dB calculated above.

Figure 3.5: Picture of HartRAO radio observatory and XDM dish with optical cable path (as adapted from [8])

3.3.3 Conclusion

The VNA has its own measuring uncertainty for gain and phase measurement. With the VNA placed in an air conditioned environment the VNA and test leads measures gain and phase with an uncertainty ± 0.13 dB and ± 2 degrees respectively.

3.4 Fibre under test - The XDM dish fibre installation

The XDM radio telescope is one of the first engineering prototypes en route to the MeerKAT telescope. It is situated at the HartRAO (Hartebeeshoek Radio Astronomy Observatory) in the Guateng province of South Africa. The XDM dish makes use of an optical link to transport RF and control information between the focus of the dish and the control room. Figure 3.5 shows an aerial picture of the observatory, showing where the XDM dish is situated and the 2 main duct lengths of the optical link. The optical fibre cable has a total length of around 250 m, giving a round trip fibre length of around 500 m.

3.5 Conclusion

This chapter describes and motivates the methods and materials used to perform the experiments in this dissertation.

The VNA measures the S21 scattering parameter of the analogue optical fibre link and internally calculates the gain and phase information with an uncertainty. The gain and

phase uncertainty of the VNA was demonstrated with an experiment which measured the drift in the measured value of an attenuator with the VNA in a room temperature environment. The gain and phase drift is strongly correlated with the room temperature and the magnitude compared well to calculated value which is based on the published specification of the VNA.

Noise Figure is measured with a Noise Figure analyser and temperature with the iButton temperature logger.

The XDM telescope is introduced and the optical fibre link length is described.

Chapter 4

Gain stability of analogue optical fibre links

This chapter contains the gain stability results and analysis of measurements made with the Photonics optical transmitter and receiver. Two tests were performed: 1) gain stability of the optical fibre when subjected to temperature changes inside a temperature chamber and 2) gain stability of the Photonics link with a short length of fibre. Then using these results the expected gain change over 10 minutes (i.e. gain stability) of the optical fibre link, in the physical environment defined in Section 2.4, is calculated. The chapter concludes with practical measurements of the gain stability of the XDM optical fibre link during sunset and during movement of the dish.

4.1 Gain stability with temperature of optical fibre (long fibre)

In this experiment a 4260 m length of fibre rolled into a spool is subject to temperature changes inside a temperature chamber. The goal of this experiment is to measure the gain stability of optical fibre when subjected to temperature changes.

4.1.1 Experiment setup

1. The fibre spool is placed inside a temperature chamber.
2. The Photonics transmitter and receiver is placed outside the chamber and connected to the fibre spool with 2x 2m patch cords via a port on the side of the chamber.
3. Gain @ 2 GHz is measured using a VNA attached to the transmitter and receiver using the test configuration in Figure 3.3.
4. The Labview script records the gain measurement of the link at 5 s intervals for 30 minutes

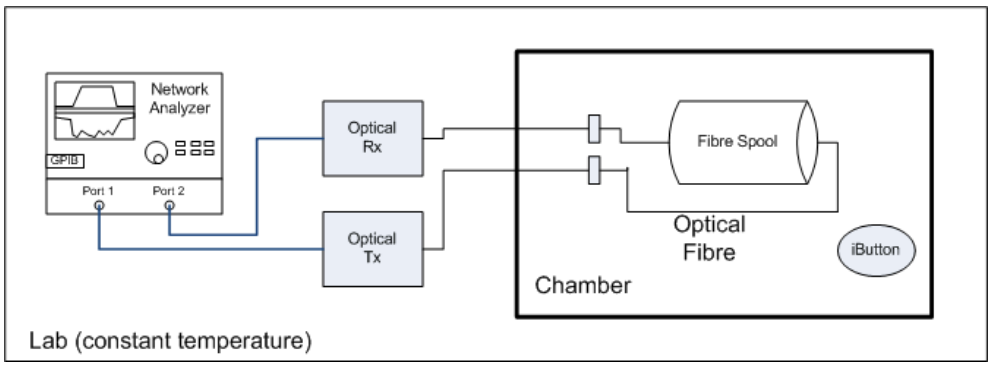

Figure 4.1: Experimental setup measuring the gain variations @ 2 GHz of an optical link when subjecting the optical fibre portion (4km spool) to temperature changes inside a temperature chamber

Table 4.1: Summary of experimental uncertainties in the experiment to determine the gain stability of optical fibre with temperature using a fibre spool

Measured/Calculated parameter	Uncertainty source and value	Uncertainty
gain [dB]	VNA, $\pm$0.13	2.5 %
optical fibre length [km]	OTDR, 1%	1 %
temperature [C]	iButton, $\pm$0.5	2.5 %
gain/length/temperature [dB / km / C]	VNA, OTDR, iButton	6 %

5. The temperature in the chamber is logged using the iButton at 30 s intervals.

6. This setup is shown in Figure 4.1.

4.1.2 Experimental uncertainty of measurement setup

The VNA is at lab temperature, thus the gain uncertainty of $\pm$0.13 dB is assumed. The Photonics transmitter and receiver has a zero mean gain change over the duration of the experiment with an uncertainty of $\pm$0.04 dB[1] . The 2x 2 m of optical fibre patch cord has an very small effect compared to the 4260 m of optical fibre and will be ignored.

The optical fibre spool length was measured using an OTDR. The specific OTDR used is not known, but it is assumed to measure length with an accuracy of 1 %.[2]

The iButton temperature sensor has an uncertainty of $\pm$0.5 C.

This information is summarised in Table 5.1.

4.1.3 Results

Figure 4.2 shows the temperature and gain results of this experiment.

[1] $\triangle$2 C x 0.02 dB/C when using the potential $\triangle$2 C of the lab environment and using the result of the OTx-ORx stability measured in Section 4.2

[2] Typical OTDR uncertainty as taken from Wikipedia - Optical time-domain reflectometer,

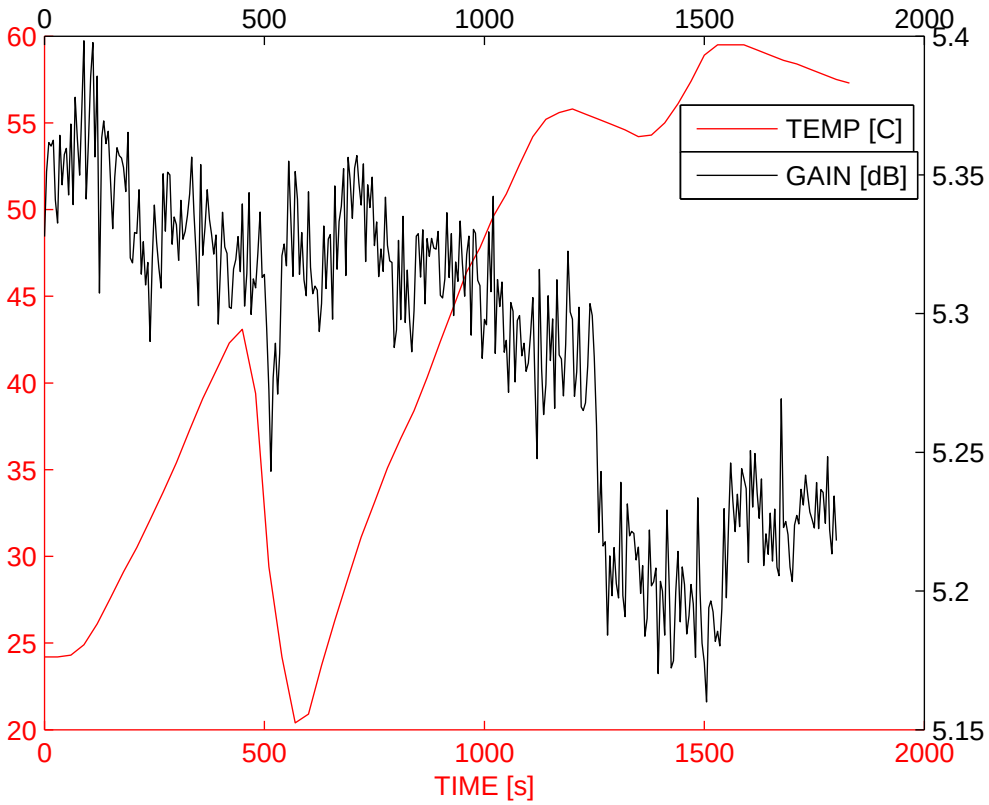

Figure 4.2: Temperature and gain @ 2 GHz of fibre spool placed inside a temperature chamber to determine the gain stability of the optical fibre with temperature

4.1.4 Results analysis

The thermal chamber had a poor temperature stability and thus a stable temperature set point could not be attained. Due to this poor stability of the thermal chamber and the low thermal mass of the fibre spool it was difficult to choose specific temperatures for this experiment[3]. To circumvent this problem an area on the result graph is chosen where the gain and temperature changes linearly, so that the ratio of the two plots would be the gain stability with temperature. The linear region chosen is between 700 and 1200 s. Figure 4.3 shows the linear region and the curves fitted to the plots in that region.

The gradient for temperature in that region is 0.052 C/s, while that of the gain is -0.00010 dB/s. The gain stability of the optical fibre with temperature is thus -0.0019 dB/C. This equates to a gain stability per kilometre of -0.00045 dB/km/C $\pm$0.00003 dB.

http://en.wikipedia.org/wiki/Optical_time-domain_reflectometer, accessed 18/08/2009

[3]Even though the iButton was placed outside of the air flow of the chamber fan and in a location that is a best guess to be representative of the air temperature of the chamber when the chamber fan is off. The fibre spool has a low thermal mass and for purposes of this experiment is assumed to be equal to the temperature of the temperature sensor. It would have been better to put the spool inside a box inside the temperature chamber and measure the temperature inside the box.

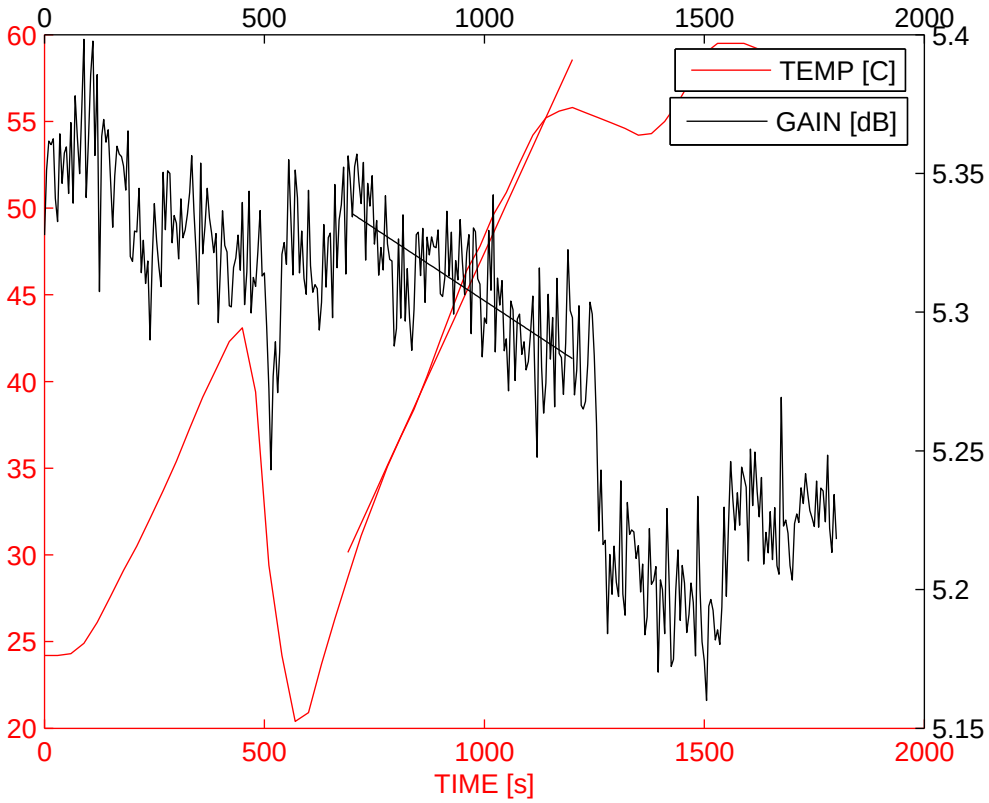

Figure 4.3: Linear region chosen to fit straight line curves to the gain and temperature plots. The gradients of these curves will be used to calculate the gain stability of optical fibre spool with temperature changes

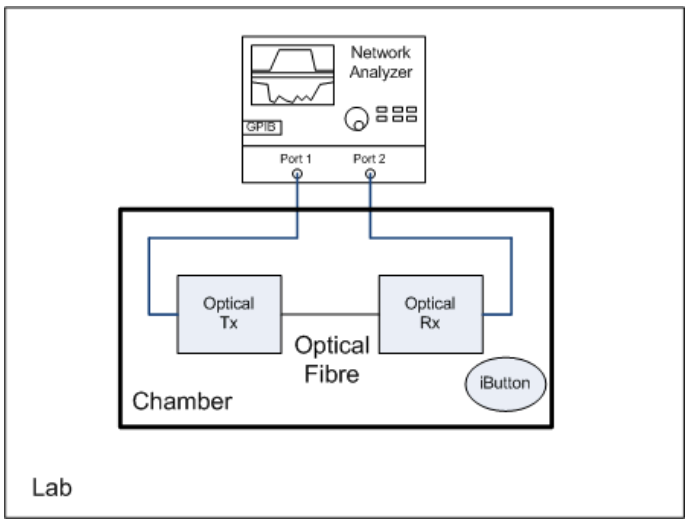

Figure 4.4: Experiment setup to determine gain stability of optical link (short fibre length)

4.1.5 Conclusion

The gain stability with temperature of a 4260 m length of optical fibre wound onto a spool and subjected to temperature changes inside a thermal chamber has been measured. This gives an indication of the gain-length-temperature coefficient of fibre which has been calculated to be -0.00045 dB/km/C $\pm$ 0.00003 dB.

4.2 Gain stability of optical link (short fibre length)

This section sets out to measure the gain stability of the optical transmitter and receiver parts of the link with changes in temperature. This is achieved by measuring the gain of the optical transmitter and receiver placed together inside a temperature chamber[4]. A short length of fibre is used so that the fibre makes an insignificant contribution to the measured gain stability.

4.2.1 Experiment setup

1. The Photonics transmitter and receiver is linked via a 2 m optical fibre pigtail.
2. The optical link is placed in a temperature chamber and connected to the VNA via coaxial cable through a side port of the chamber.
3. Temperature was measured with the iButton.
4. Due to the poor temperature stability of the chamber the optical link could only be measured at 4 temperatures. The gain @ 2 GHz was measured at the following

[4]The optical transmitter and receiver gain stabilities are measured as one parameter in this experiment. It would have been more useful to measure the gain stability with only the transmitter and only the receiver as in practice the transmitter and receiver are in different locations.

chamber temperatures: [20.5, 24.5, 34.0, 35.0] C. The gain values are measured only once the gain values on the VNA display has stabilised as seen by the eye.

5. This setup is shown in Figure 4.4.

4.2.2 Experimental uncertainty of measurement setup

Using the optical fibre RF gain variation versus temperature relationship of 0.0014 dB/km/C deduced in Section 2.3.1 a RF gain change contribution of about 42×10^{-6}dB is expected from a 2 m length of fibre with the 15 C variation in the temperature chamber. The VNA is in the lab environment thus has an uncertainty of 0.13 dB. The total gain uncertainty of the experiment is thus: optical fibre patch lead uncertainty + VNA uncertainty = $\pm$0.13 dB.

The temperature sensor has an uncertainty of $\pm$0.5 C[5]. These uncertainties are summarised in Table 5.2[6].

Table 4.2: Uncertainties of experiment to measure gain stability of the optical link (short fibre length) with temperature

Measured/Calculated Parameter	Uncertainty source and value 1	Uncertainty source and value 2	Total Uncertainty
Gain [$\pm$dB]	VNA 0.03 (Assuming temperature around VNA is constant)	Optical fibre test lead 42×10^{-6}	4.3 %
Temperature [$\pm$C]	iButton 0.5	–	2.5 %
gain/temp stability [dB / C]	gain	temperature	6.8 %

4.2.3 Experiment results

Figure 4.5 shows the gain versus temperature plot. This results are listed in the Table 4.3.

[5]Also, the effective temperature of the optical Tx and Rx unit is not known accurately as the temperature sensor only measures the air temperature in the chamber at a region local to the units. The units do however have a solid stainless steel (modules weigh close to 500 g each) chassis so the effective temperature is expected to change slowly and this thermal lag effect is minimised by taking the measurement once the gain value on the VNA display had stabilised as seen with the eye on the VNA display.

[6]Note that the fractional uncertainty is calculated using the rule: fractional uncertainty of a/b = sum of fractional uncertainties of a and b. Here worst case fractional uncertainties are used

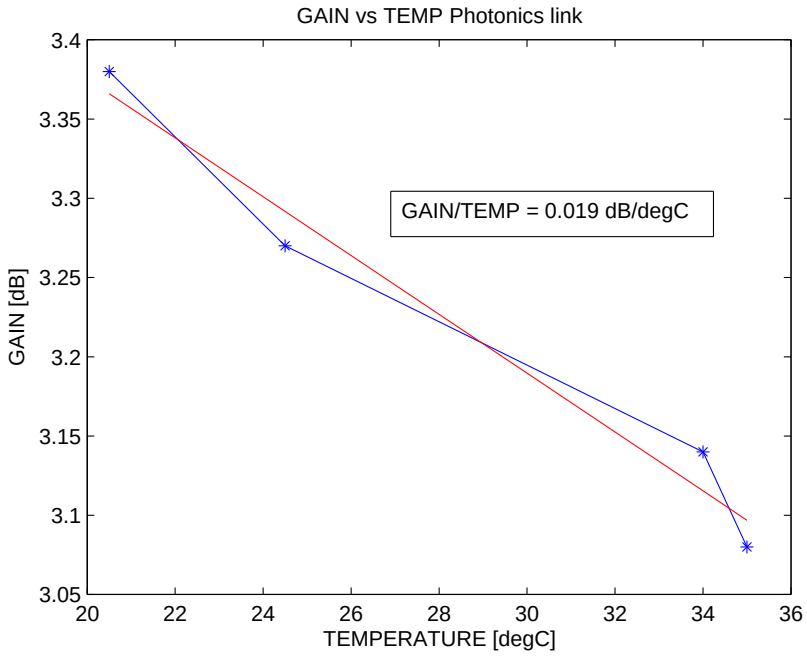

Figure 4.5: GAIN changes versus temperature for Photonics link (short fibre length) placed inside a temperature chamber to determine the gain stability of the link. (Raw data is BLUE, while fitted data in RED)

Table 4.3: Table of gain changes with temperature of Photonics link (short fibre length) to determine gain stability of link with temperature

TEMP [C]	GAIN [dB]
20.5	3.38
24.5	3.27
34.0	3.14
35.0	3.08

4.2.4 Results analysis

The dataset consist of only 4 points, so it is not possible to make precise conclusion about the gain-temperature coefficient. The trend however indicates that the gain decreases with rising temperature. Assuming the result of -0.019 $\pm$ 0.001 dB/C then an environment with a temperature stability of 1.5 C over 10 minutes is required if the Photonics link is to be utilised. Better than 1 degree of temperature stability over 10 minutes is easy to provide using peltier, water cooling, or if practical constraints allow, mounting the optical transmitter and receiver on a thick enough plate.

Note that the thermal mass of the photonics units have not been considered in this analysis and will further relax the temperature stability requirements of the environment.

Gain stability data was not available from Photonics so a result comparison can not be made

4.2.5 Conclusion

The gain stability of the analogue optical transmitter-receiver pair, connected by 1 m of fibre and subjected to temperature changes inside a chamber, has been measured. The link has a gain-temperature coefficient of -0.019 $\pm$ 0.001 dB/C.

4.3 The gain stability of the RF over fibre link in the KAT-7 environment

In Section 2.4 a thermal environment is defined that is based on the KAT-7 environment. Using the measured results of gain stability with temperature of the optical fibre and the transmitter and receiver contained in this chapter, the expected gain changes will now be calculated for the defined environment. The results of this will be used to determine whether an analogue optical fibre link can meet the requirement for gain stability for KAT-7 and other radio telescopes using a similiar configuration. Table 4.4 shows the result.

The $\triangle gain$ over 10 minutes calculated as 0.038 dB. Even though this is marginally by (0.01 dB) over the requirement the assumption of the temperature change on the cold plate was during the unlikely event of the water temperature changing by 2 C over 10 minutes. In addition, the KAT-7 system has peltiers which control the temperature much tightly. The gain stability of the optical link is thus a PASS.

Table 4.4: Table calculating the various components contributing to the gain stability of the link defined in Section 2.4. The total gain change will be evaluated against the KAT-requirement.

Optical link component	Gain calculation	Gain contribution [dB] in 10 minutes
Transmitter and Receiver	$\triangle gain$= (gain stability of OTx and ORx)$\triangle T$ = (0.019 dB/C)(2 C)	0.038
Underground optical fibre (6 km)	$\triangle gain$= (length)(gain stability of fibre)$\triangle T$ = (5 km)(0.00045 dB/km/C)(1e-6 C)	2×10^{-9}
Transitional optical fibre (30 m)	$\triangle gain$ = (length)(gain stability of fibre)$\triangle T$ = (0.01 km)(0.00045 dB/km/C)(0.28 C)	1×10^{-6}
Total gain change in 10 minutes	Sum of the different gain contributions	0.038

4.4 Gain stability of optical fibre installation of the XDM optical link during sunset

In this experiment the gain change of the XDM optical fibre installation is measured during sunset[7]. This information is used to calculate the gain stability with temperature of the XDM link which consists of an analogue optical transmitter and an optical receiver at the ends of a fibre length of around 500 m. The objective of this chapter is to give the reader an idea of the degree of gain stability one can expect from a RF-over-fibre link in a real radio telescope installation.

4.4.1 Experiment setup

1. The Photonics transmitter and receiver is connected to the XDM link using two 2 m patch cables.

2. Using the test configuration of Figure 3.3 with the DUT being the optical link described above. The experiment was setup to record data at 1 minute intervals for 5 hours.

3. The VNA measured gain @ 2 GHz

4. Experiments ran for a 5 hour period between 16h26 to 21h26 as this was the time when the temperature changed most rapidly. The selection of these intervals was

[7]Similiar measurements were also made of the link during sunrise. Due to the temperature sensor (as well as parts of the optical fibre cable) being in direct sunlight and as a result reports inflated readings, it will be excluded from the analysis.

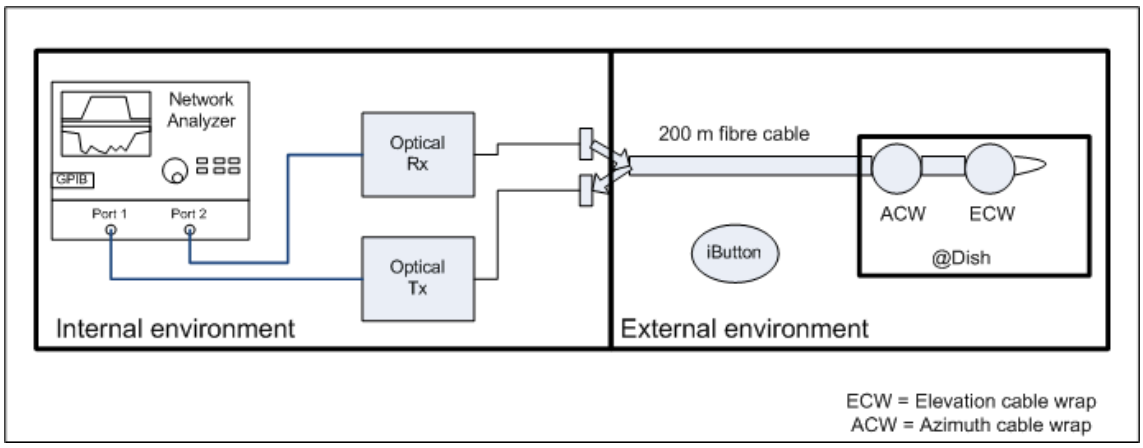

Figure 4.6: Test setup to measure gain stability with temperature of the XDM installation during sunset

Table 4.5: Summary of experimental uncertainties in the experiment to determine the gain stability with temperature of the XDM optical fibre link

Measured/Calculated parameter	Uncertainty source and value	Uncertainty %
Gain [dB]	VNA, $\pm$0.13	2.5 %
Temperature @ dish ambient [C]	iButton, $\pm$0.5	7.1 %
gain/temperature [dB / C]	calculation	9.6 %

based on the environmental data of the preceding few days as measured by the HartRAO weather station. This data is shown in Figure 4.8.

5. Temperature measurements were made with an iButton located in the ambient close to the dish at 1 minute intervals for the duration of the experiment.

6. For these measurements the dish points towards Zenith

7. The test setup is shown in Figure 4.6.

4.4.2 Experimental uncertainty of measurement setup

With the VNA in the lab environment the gain measurements have an uncertainty of $\pm$0.13 dB. The ambient temperature is measured in the vicinity of the dish with an iButton and has a temperature uncertainty of $\pm$0.5 C.

Using the above information the uncertainty for the gain stability measurement with temperature of the XDM link is calculated as 10 %

This uncertainty information is summarised in the Table 4.5.

4.4.3 Experiment results

The sunset data is shown in Figure 4.7.

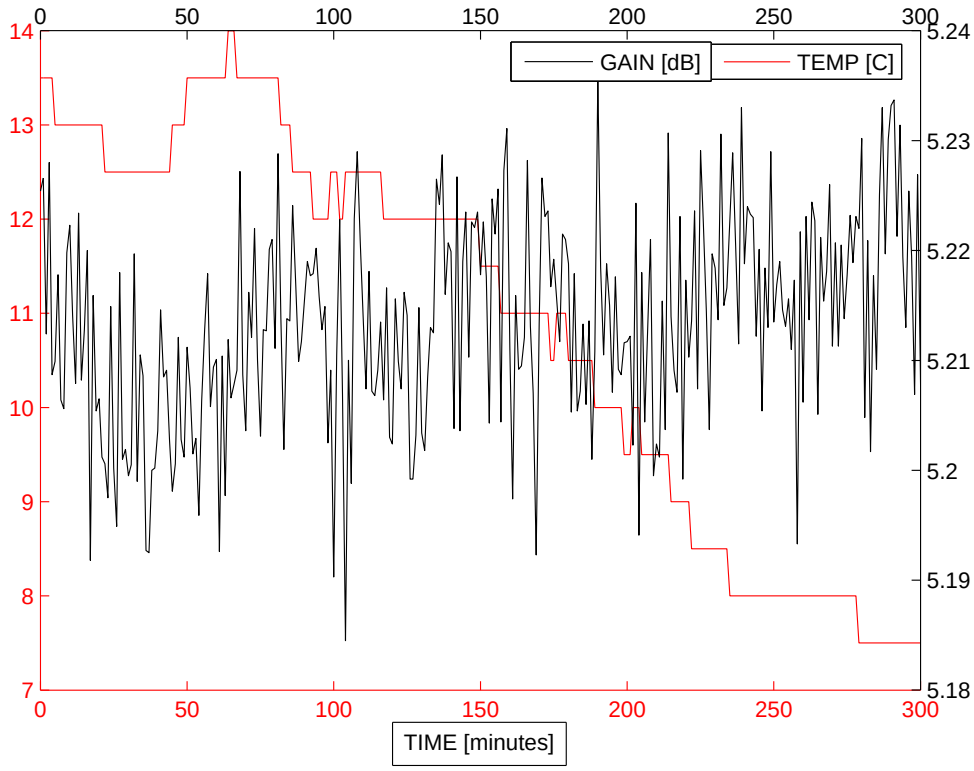

Figure 4.7: Measurements of gain change @ 2 GHz of XDM optical link and temperature during sunset

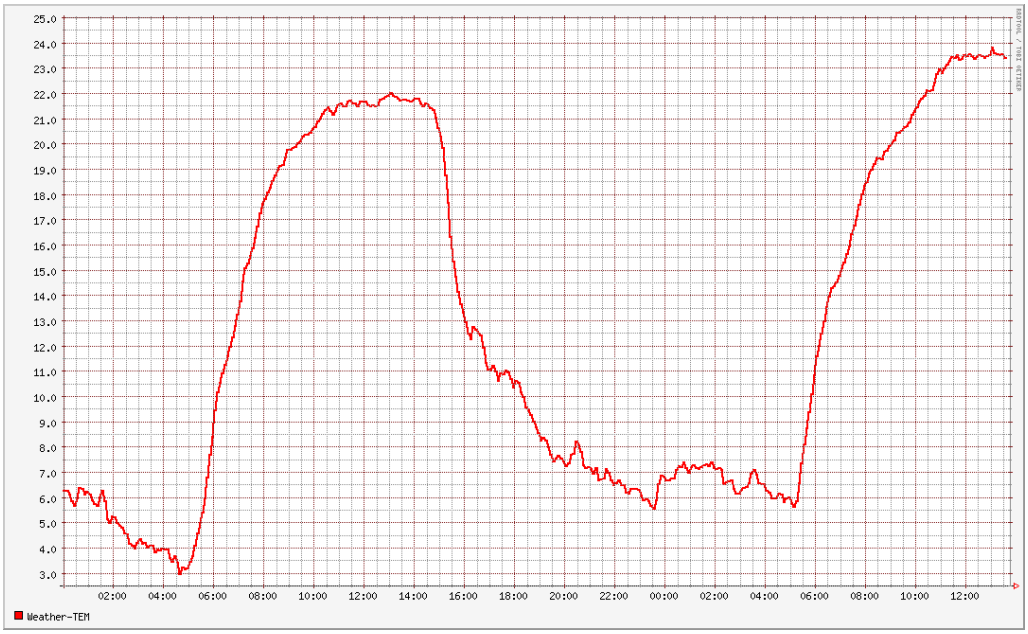

Figure 4.8: HartRAO air temperature for preceding 2 days before experiment

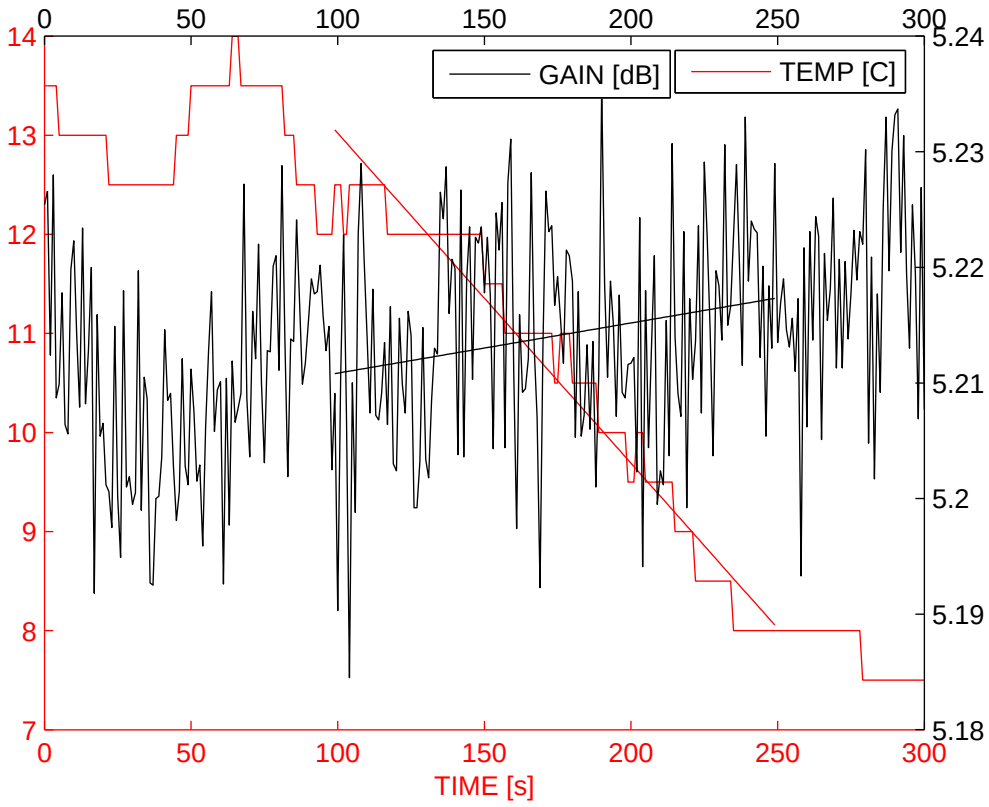

Figure 4.9: Linear regions chosen where the gain and temperature changes linearly with time during sunset to determine the gain stability of the XDM optical link

4.4.4 Results analysis

As expected we see that the gain has a negative slope with temperature. To calculate the gain stability, sections of the graph are chosen where the temperature and gain plots are linear. A straight line is then fitted to these linear sections of the gain and temperature plots and the ratio of the gradients of the gain to the temperature fit equals the gain stability of the optical fibre link with temperature.

Between 100 and 250 minutes the gain gradient is 43×10^{-6}dB/minute and the temperature gradient is -0.033 C/minute. Figure 4.9 shows the temperature and gain plots with the fitted lines.

The gain stability for the XDM optical fibre link is thus calculated to be -0.0013 dB/C $\pm$0.0001 dB. This equates to worst case gain change of -0.00043 $\pm$0.00003 dB over 10 minutes in the month[8] that the optical link was measured.

4.4.5 Conclusion

The gain stability of the XDM optical fibre installation has been measured during sunset. The link has a gain stability of -0.0013 dB/C $\pm$0.0001 dB which results in a gain change

[8]The link was measured during June 2008. This is a Winter month and the temperature changes are thus slower than during the warmer Summer months.

of -0.00043 dB over 10 minutes at sunset during Winter.

4.5 Gain stability during movement of the XDM dish

The azimuth and elevation movement of the dish causes bending / torsional forces on the optical fibre cable running in the horizontal and vertical cable wraps. This experiments sets out to measure the changes in gain caused by these mechanical stresses on the cable. Appendix B contains a more detailed description of the mechanism of the cable wraps used in the XDM dish.

4.5.1 Experiment setup

1. The Photonics transmitter and receiver is connected to the XDM link using 2x 2 meter patch cable

2. Experiment starts at around 2 PM when the ambient temperature rate of change is the slowest. This time period was determined from measurements of the preceding 2 days ambient temperature as illustrated in Figure 4.8.

3. For the azimuth movement measurement, the dish's elevation coordinate is fixed at 90 degrees and the azimuth position is steered to the following positions: [-160 -128, -96, -64, -32 0 , 32, 64, 96, 128, 160] degrees.

4. Readings of the gain @ 2 GHz are measured with a VNA at each azimuth position change of the dish.

5. For the elevation movement measurement, the dish's azimuth coordinate is fixed at 0 degrees and the elevation position of the dish is steered to the following positions: [90, 80, 70, 60, 50, 40, 30, 20, 10] degrees

6. Readings of the GAIN @ 2 GHz are measured with a VNA at each elevation position change of the dish.

4.5.2 Experimental uncertainty of measurement setup

Each movement run had a duration of a few minutes thus the lab temperature can be assumed to be constant during that time. The temperature component of the VNA uncertainty equation thus falls away and the VNA can be assumed to measure gain with an uncertainty of 0.03 dB. The gain changes with temperature of the optical fibre link can be assumed to be zero due to the time of day that the experiment takes place and thus does not contribute to the uncertainty.The total gain uncertainty of the experiment is thus equal to the VNA uncertainty of ± 0.03 dB

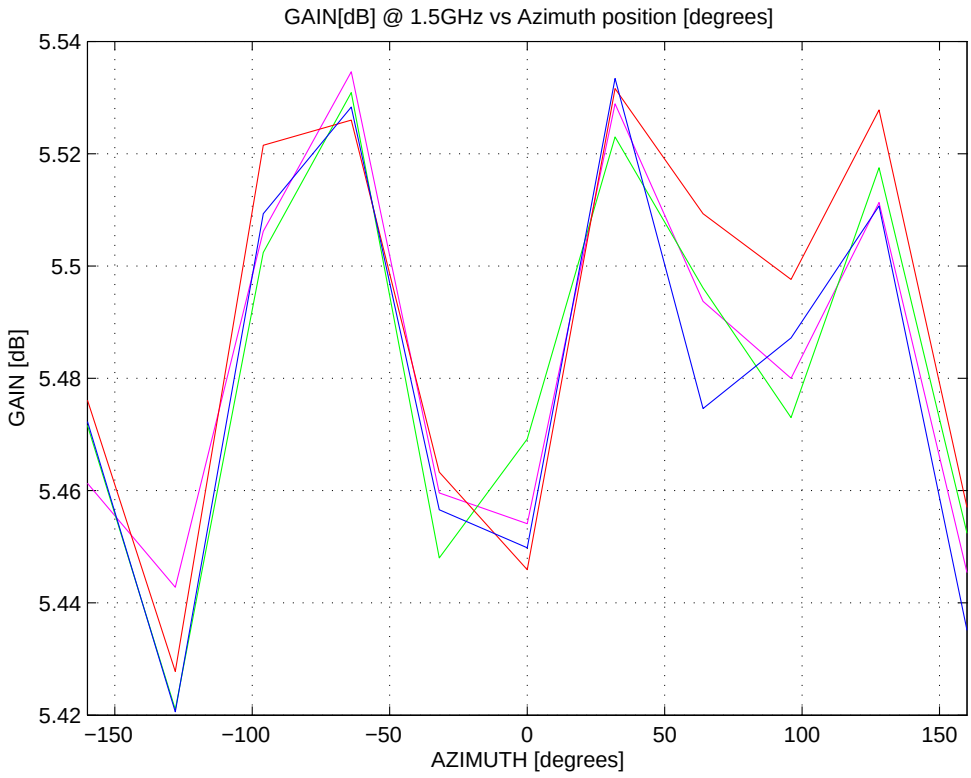

Figure 4.10: RF gain changes of optical fibre link versus azimuth angle of XDM dish for 4 runs of the experiment. Notice that the gain shape is repeatable between the different runs of the experiment

The dish position angle has an uncertainty of ±2 degrees. Radio telescopes position angles are generally accurately calibrated as it is required to locate extra-terrestial sources with arc second resolution. This uncertainty however comes about as when entering the desired angle manually the dish position (as displayed on the digital readout[9]) did not move exactly to this desired position (might have been a bug in the dish controller). This offset was also not repeatable between experiment runs and had a spread of 2 degrees.

4.5.3 Results

The gain versus Azimuth position data is shown Figure 4.10. The gain versus elevation position data is is shown in Figure 4.11.

4.5.4 Results analysis

For both azimuth and elevation the results are repeatable within the uncertainty (±0.03dB) of the VNA. The 2 degrees uncertainty in dish position does not feature since the gain changes slowly with angle (e.g. 0.06 dB between 0 and 32 degrees, thus 0.004 dB in 2

[9]The dish position readout is based on a mechanical position encoder in the dish and is the part that is calibrated. One can thus expect this reading to accurately describe the position of the dish.

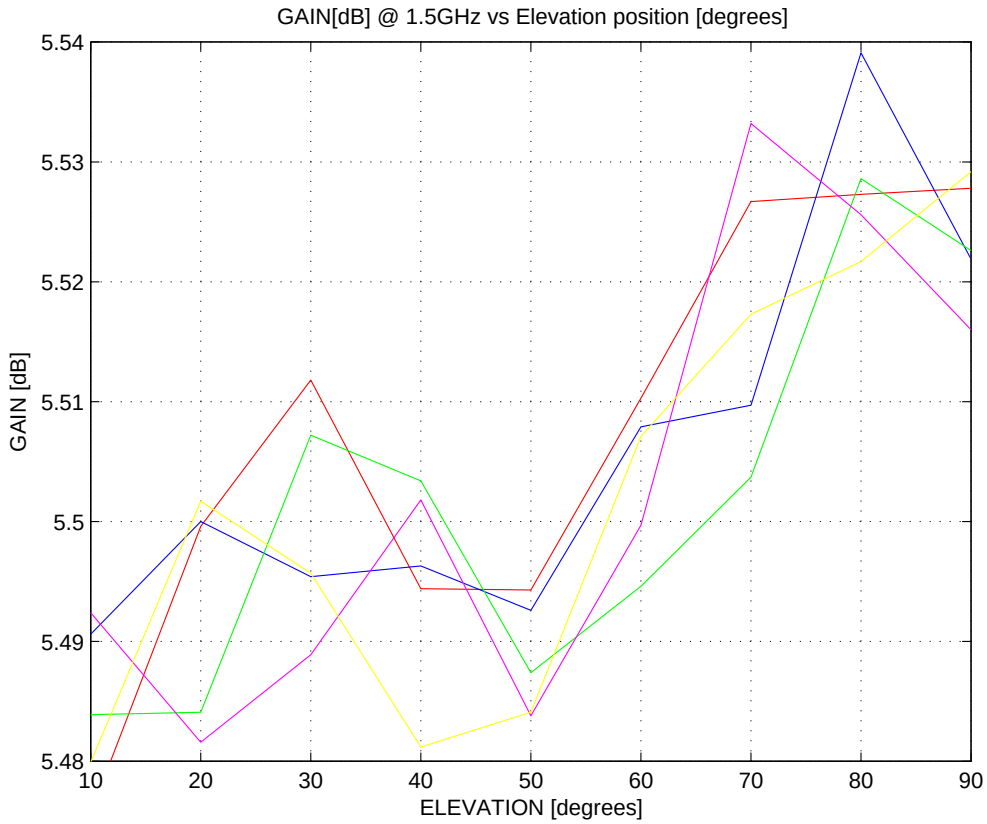

Figure 4.11: RF gain changes of optical fibre link versus elevation angle of XDM dish for 4 runs of the experiment. Notice that the gain shape is repeatable between the different runs of the experiment

degrees).

Azimuth data: The optical fibre cable has a predominantly torsional force applied to it when going either side of the unstressed position (at azimuth angle -30 degrees). Information of the physical dynamic of the optical fibre cable during azimuth movement is unavailable at the time of this analysis[10] and it is thus difficult to explain the 3 peaks in the gain profile. We can however characterise the worst case gain change over 10 degrees movement in azimuth. From the azimuth data there are increases and decreases in gain when moving from -160 to +160 degrees of azimuth position. The worst case $\triangle$gain in 10 degrees azimuth change is 0.024 $\pm$0.03 dB.

Elevation data: The gain increases with an increase in elevation position. The elevation cable wrap has a predominantly bending effect on the optical fibre cable. Optical fibre has an increase in loss with an increase in bending, so the decreasing loss with decreasing bending as the dish increases in elevation position is demonstrated. The total change in gain is 0.06 dB for 80 degrees of elevation movement. The worst case $\triangle$gain in 10 degrees is 0.025$\pm$0.03 dB

4.5.5 Additional movement experiment for dynamic behaviour

The azimuth movement was repeated to check the dynamic behaviour of the gain during azimuth movement and also to check that the position sampling in the previous experiment, of 32 degrees, captures all the information. This was achieved by programming the XDM dish control computer to do 2 cycles of azimuth movement. A Labview script was written to control the VNA to measure gain data from the Photonics link continuously (approximately 1.3 s time intervals).

Time synchronisation was achieved by programming the antenna computer to generate time stamped position data (at approximately 10 ms intervals) and modifying the Labview script to time stamp its gain data. The 2 sets of results are time aligned in Matlab.

The result of Figure 4.12 proves that the position sampling of the data in Section 4.5.3 is adequate.

4.5.6 Conclusion

GAIN changes of the HartRAO optical link were measured while the dish was moved in azimuth and elevation. The gain results for both azimuth and elevation movement were repeatable between measuring runs. The gain change of 10 degrees of azimuth and elevation movement is 0.024$\pm$0.03 dB and 0.025$\pm$0.03 dB respectively. An additional experiment is performed where the gain is sampled continuously as the XDM dish is being moved in azimuth. The shape of the resultant gain plot is similiar as with the previous experiment.

[10] Analysing the exact movement of the cable in the azimuth cable wrap was not deemed important at the time of measurement.

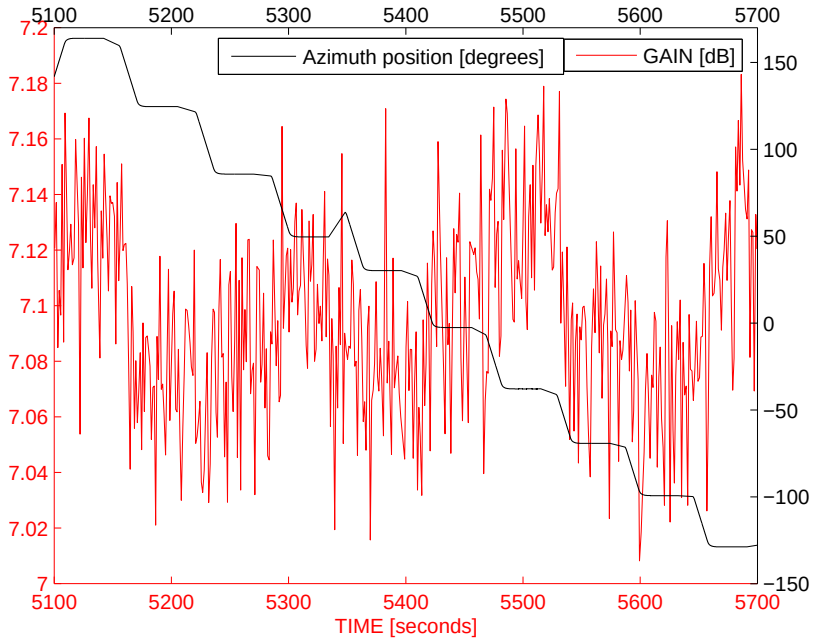

Figure 4.12: Gain [dB] over one cycle of azimuth over time. The same peaks are visible at the same azimuth positions as with the previous data. The roughness of the plot is an indication of the ± 0.03dB measuring uncertainty of the VNA

4.6 Conclusion

In this chapter the gain stability of an analogue optical fibre link with temperature was measured. This was done by setting up experiments to measure the gain stabilities of the optical transmitter-receiver and of the optical fibre. The results of these individual portions of the link were combined in a calculation to check the gain change over 10 minutes (i.e. gain stability) of an analogue optical link inside a thermal environment based on the KAT-7 environment. The gain stability of the analogue optical fibre link is found to be sufficiently stable to pass the KAT-7 apportioned requirements. Further experiments for antenna movement and environmental temperature swings (such as happens during sunset) were performed on the XDM link for additional practical data.

Chapter 5

Phase stability of analogue optical fibre link

This chapter contains the phase stability results and analysis of measurements made with the Photonics optical transmitter and receiver. Two tests were performed: 1) Phase stability of the optical fibre when subject to temperature changes inside a temperature chamber and 2) phase stability of the Photonics link with a short length of fibre. Using these results the expected phase change over 10 minutes (i.e. phase stability) of the optical fibre link, in the physical environment defined in Section 2.4, is calculated. The chapter concludes with practical measurements of the phase stability of the XDM optical fibre link during sunset and during movement of the dish.

5.1 Phase stability of optical fibre when inside a temperature chamber

In this experiment a 4260 m length of fibre rolled into a spool is subject to temperature changes inside a temperature chamber. The goal of this experiment is to measure the phase stability of optical fibre when subjected to temperature changes.

5.1.1 Experiment setup

1. The fibre spool is placed inside a temperature chamber.
2. The Photonics transmitter and receiver is placed outside the chamber and connected to the fibre spool with 2x 2m patch cords via a port on the side of the chamber.
3. Phase @ 2 GHz is measured using a VNA attached to the transmitter and receiver using the test configuration in Figure 3.3.
4. The Labview script records the phase measurement of the link at 5 s intervals for 30 minutes

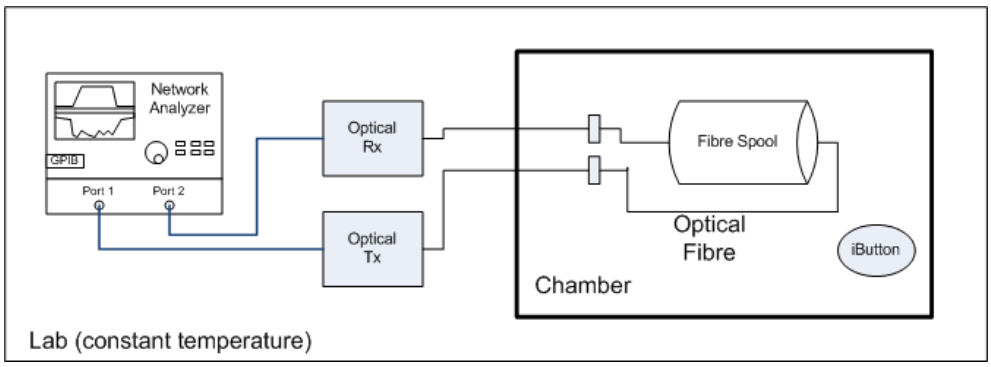

Figure 5.1: Experimental setup when measuring the RF phase variations of an optical link when subjecting the optical fibre portion (4km spool) to temperature changes inside a temperature chamber

Table 5.1: Summary of experimental uncertainties in the experiment to determine the phase stability of optical fibre using a fibre spool

Measured/Calculated parameter	Uncertainty source and value	Uncertainty
phase [degrees]	VNA, ± 2	1 %
optical fibre length [km]	OTDR, 1%	1 %
temperature [C]	iButton, ± 0.5	1 %
gain/length/temperature [degrees / km / C]	VNA, OTDR, iButton	3 %

5. The temperature in the chamber is logged using the iButton at 30 s intervals.

6. This setup is shown in Figure 5.1.

5.1.2 Experimental uncertainty of measurement setup

The VNA is at lab temperature, thus the phase uncertainty of ± 2 degrees is assumed. In the lab environment the optical transmitter and receiver is assumed to make an insignificant contribution to the phase and will be ignored. The 2x 2 m of optical fibre patch cord has an very small effect compared to the 4260 m of optical fibre and will be ignored.

The optical fibre spool length was measured using an OTDR. The specific OTDR used is not known, but it is assumed to measure length with an accuracy of 1 %.[1]

The iButton temperature sensor has an uncertainty of ± 0.5 C.

This information is summarised in Table 5.1.

5.1.3 Results

Figure 5.2 shows the temperature and phase result of this experiment.

[1]Typical OTDR uncertainty as taken from Wikipedia - Optical time-domain reflectometer, http://en.wikipedia.org/wiki/Optical_time-domain_reflectometer, accessed 18/08/2009

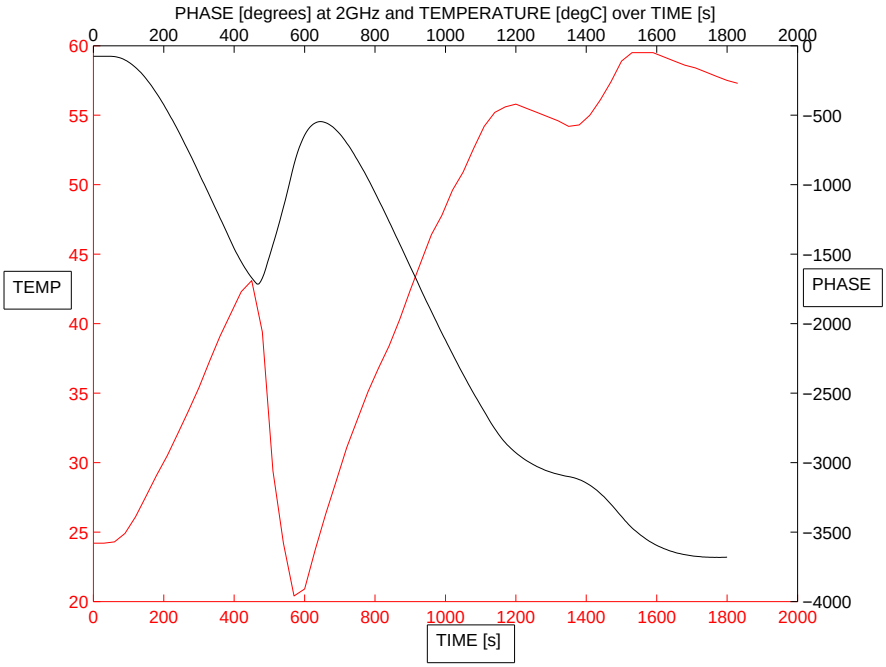

Figure 5.2: Temperature and RF phase @ 2 GHz when subjecting a fibre spool to temperature changes in side a temperature chamber

5.1.4 Results analysis

The thermal chamber had a poor temperature stability and thus a stable temperature set-point could not be attained. Due to this poor stability of the thermal chamber and the low thermal mass of the fibre spool it was difficult to choose specific temperatures for this experiment[2]. To circumvent this problem an area on the result graph is chosen where the phase and temperature changes linearly, so that the ratio of the two plots would be the phase stability with temperature. The linear region chosen is between 700 and 1200 s. Figure 5.3 shows the linear region and the curves fitted to the plots in that region.

The gradient for temperature in that region is 0.052 C/s, while that of the phase is -4.9 degrees/s. The phase stability of the optical fibre with temperature is thus -88 degrees/C. This equates to a phase stability per kilometre of -20 $\pm$1 degrees/km/C.

5.1.5 Conclusion

The phase stability of the optical fibre length wound onto a spool as been measured. This give an indication of the phase-length-temperature coefficient of fibre which is calculated to be -20 $\pm$1 degrees/km/C

[2]Even though the iButton was placed outside of the air flow of the chamber fan and in a location that is a best guess to be representative of the air temperature of the chamber when the chamber fan is off. The fibre spool has a low thermal mass and for purposes of this experiment is assumed to be equal to the temperature of the temperature sensor. It would have been better to put the spool inside a box inside the temperature chamber and measure the temperature inside the box.

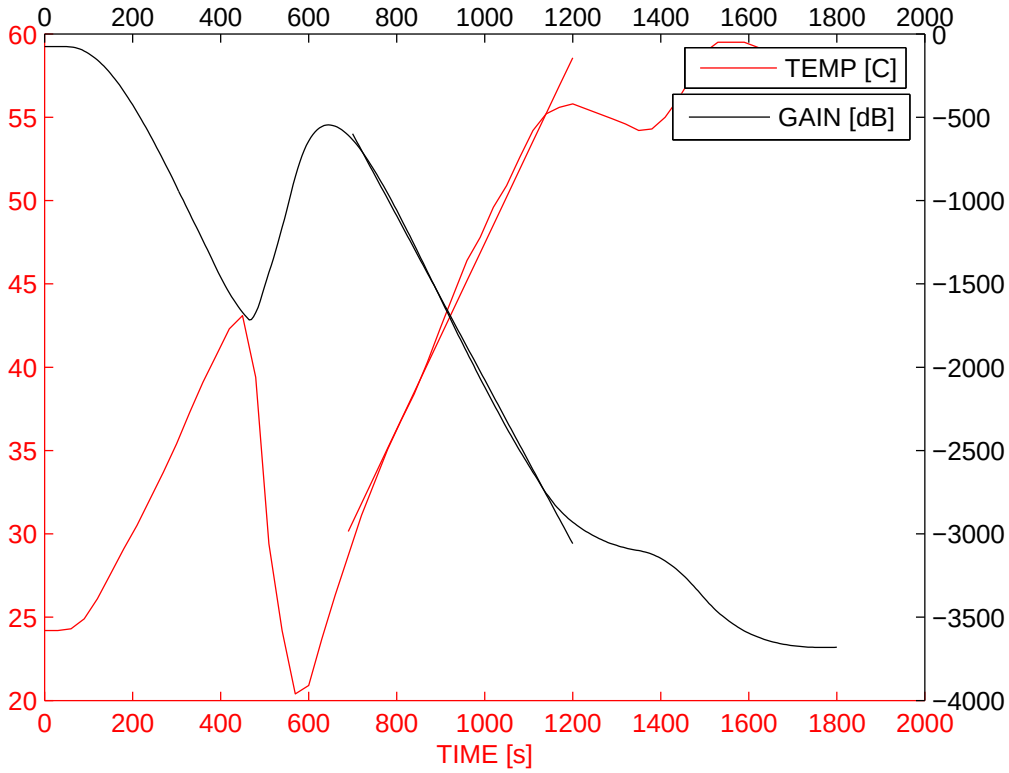

Figure 5.3: Linear region chosen and curves fitted to calculate the phase stability of optical fibre spool with temperature

5.2 Phase stability of optical link with short length of fibre

This section sets out to measure the phase stability of the optical transmitter and receiver parts of the link. This is achieved by measuring the phase of the optical transmitter and receiver placed together inside a temperature chamber[3]. A short length of fibre is used so that the fibre makes a small contribution to the measured phase stability.

5.2.1 Experiment setup

1. The Photonics transmitter and receiver is linked via a 2 m optical fibre pigtail.
2. The optical link is placed in a temperature chamber and connected to the VNA via coaxial cable through a side port of the chamber.
3. Temperature was measured with the iButton.
4. Due to the poor temperature stability of the chamber the optical link could only be measured at 4 temperatures. The phase @ 2 GHz was measured at the following

[3]The optical transmitter and receiver phase stabilities are measured as one parameter in this experiment. It would have been more useful to measure the phase stability with only the transmitter and only the receiver as in practice the transmitter and receiver are in different locations.

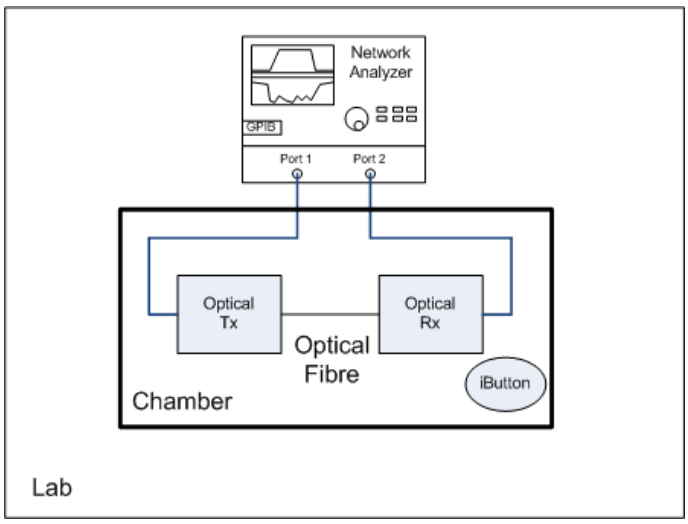

Figure 5.4: Experiment setup to determine phase stability of optical link (short fibre length) with temperature

chamber temperatures: [20.5, 24.5, 34.0, 35.0] C. The phase values are measured only once the phase values on the VNA display has stabilised as seen by the eye.

5. This setup is shown in Figure 5.4

5.2.2 Experimental uncertainty of measurement setup

Using the optical fibre RF phase variation versus temperature relationship measured in Section 5.1 a RF phase change contribution of about 0.6 degrees is expected from a 2 m length of fibre with the 15 C variation in the temperature chamber. The VNA is in the lab environment thus has an uncertainty of 2 degrees. The total phase uncertainty of the experiment is thus: optical fibre patch lead uncertainty + VNA uncertainty = $\pm(0.9 + 2)$ = ± 2.9 degrees. A phase uncertainty not accounted for is the portion of the coaxial cable which is inside the chamber.

The temperature sensor has an uncertainty of ± 0.5 C[4]. These uncertainties are summarised in Table 5.2[5].

[4]Also, the effective temperature of the optical Tx and Rx unit is not known accurately as the temperature sensor only measures the air temperature in the chamber at a region local to the units. The units do however have a solid stainless steel (modules weigh close to 500 g each) chassis so the effective temperature is expected to change slowly and this thermal lag effect is minimised by taking the measurement once the phase value on the VNA display had stabilised as seen with the eye on the VNA display.

[5]Note that the fractional uncertainty is calculated using the rule: fractional uncertainty of a/b = sum of fractional uncertainties of a and b. Here worst case fractional uncertainties are used

Table 5.2: Uncertainties of experiment to measure gain stability of the optical link (short fibre length) with temperature

Measured/Calculated Parameter	Uncertainty source and value 1	Uncertainty source and value 2	Total Uncertainty
Phase [±degrees]	VNA 2	Optical fibre test lead 0.9	130 %
Temperature [±C]	iButton 0.5	–	2.5 %
gain/temp stability [dB / C]	gain	temperature	133 %

5.2.3 Experiment results

This results are listed in the following table:

Temperature [C]	Phase [degrees]
20.5	130
24.5	131
34	132
35	132

5.2.4 Results analysis

In this experiment a phase change of 2 degrees with 15 C change in temperature is observed. The phase stability with temperature of the OTx-ORx is thus 0.1±0.1 degrees/C. From the magnitude of the uncertainty it is possible that this change can be entirely due to the VNA and the fibre patch lead and not from the optical transmitter and receiver.

As the optical fibre transmitter and receiver will be in a relatively temperature stable environment (certainly not △15 C) the phase stability effects are expected to be insignificant.

5.2.5 Conclusion

The phase stability with temperature of the analogue optical transmitter-receiver pair has been measured. The experiment measured the OTx-ORx pair to have a phase stability of 0.1 degrees/C. When considering that the optical transmitter and receiver is in a temperature stabilised environment it adds an insignificant amount to the phase stability of the system

Table 5.3: Table calculating the various components contributing to the phase stability of the link defined in Section 2.4. The total phase change will be evaluated against the KAT-requirement.

Optical link component	Phase calculation	Phase contribution [degrees] over 10 minutes
Transmitter and Receiver	$\triangle phase$ = (phase stability of OTx-ORx [degrees/C])$\triangle T$ = (0.1)(2)	0.2
Underground optical fibre (6 km)	$\triangle phase$ = (phase stability of optical fibre)(length)$\triangle T$ = (-20 [degrees/km/C])(5 [km])(1e-6 C)	0.0001
Transitional optical fibre (30 m)	$\triangle phase$ = (phase stability of optical fibre [degrees/km/C])(length [km])$\triangle T$ = (-20)(0.01)(0.28)	0.06
TOTAL	Sum of the different phase contributions	0.26

5.3 The phase stability of the RF over fibre link in the KAT-7 environment

In Section 2.4 a thermal environment was defined that is based on the KAT-7 environment. Using the measured results of phase stability with temperature of the optical fibre and the transmitter and receiver contained in this chapter, the expected phase changes will now be calculated for the defined environment. The results of this will be used to determine whether an analogue optical fibre link can meet the requirement for phase stability in the KAT-7 environment. Table 5.3 is the result. The calculated phase change of 0.26 degrees is almost 8 times better than the KAT-7 requirement.

5.4 Phase stability of optical fibre installation of the XDM optical link during sunset

In this experiment the phase change of the XDM optical fibre installation is measured during sunset[6]. This information is used to calculate the phase stability with temperature of the XDM link which consists of an analogue optical transmitter and an optical receiver at the ends of a fibre length of around 500 m. The objective of this chapter is to give the reader an idea of the degree of phase stability one can expect from a RF-over-fibre link in

[6]Similiar measurements were also made of the link during sunrise. Due to the temperature sensor (as well as parts of the optical fibre cable) being in direct sunlight and as a result reports inflated readings, it will be excluded from the analysis.

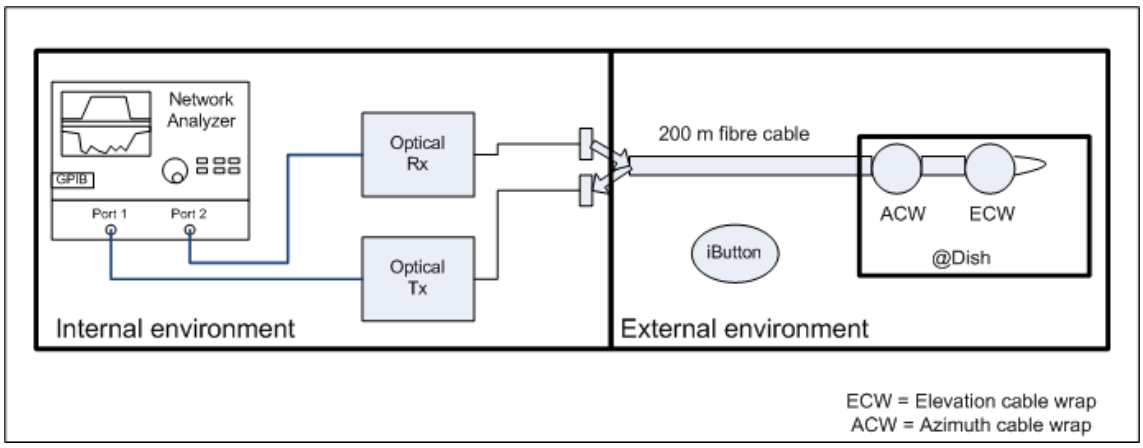

Figure 5.5: Test setup to measure phase stability with temperature of the XDM optical fibre installation during sunset

a real radio telescope installation.

5.4.1 Experiment setup

1. The Photonics transmitter and receiver is connected to the XDM link using two 2 m patch cables.
2. Using the test configuration of Figure 3.3 with the DUT being the optical link described above. The experiment was setup to record data at 1 minute intervals for 5 hours.
3. The VNA measured phase @ 2 GHz
4. Experiments ran for a 5 hour period between 16h26 to 21h26 as this was the time when the temperature changed most rapidly. The selection of this intervals was based on the environmental data of the preceding few days as measured by the HartRAO weather station. This data is shown in Figure 4.8.
5. Temperature measurements were made with an iButton located in the ambient close to the dish at 1 minute intervals for the duration of the experiment.
6. For these measurements the dish points towards Zenith
7. The test setup is shown in Figure 5.5.

5.4.2 Experiment uncertainty of measurement setup

The VNA is at lab temperature, thus the phase uncertainty of ± 2 degrees is assumed. In the lab environment the optical transmitter and receiver is assumed to make an insignificant contribution to the phase and will be ignored. The 2x 2m patch cords is in a lab

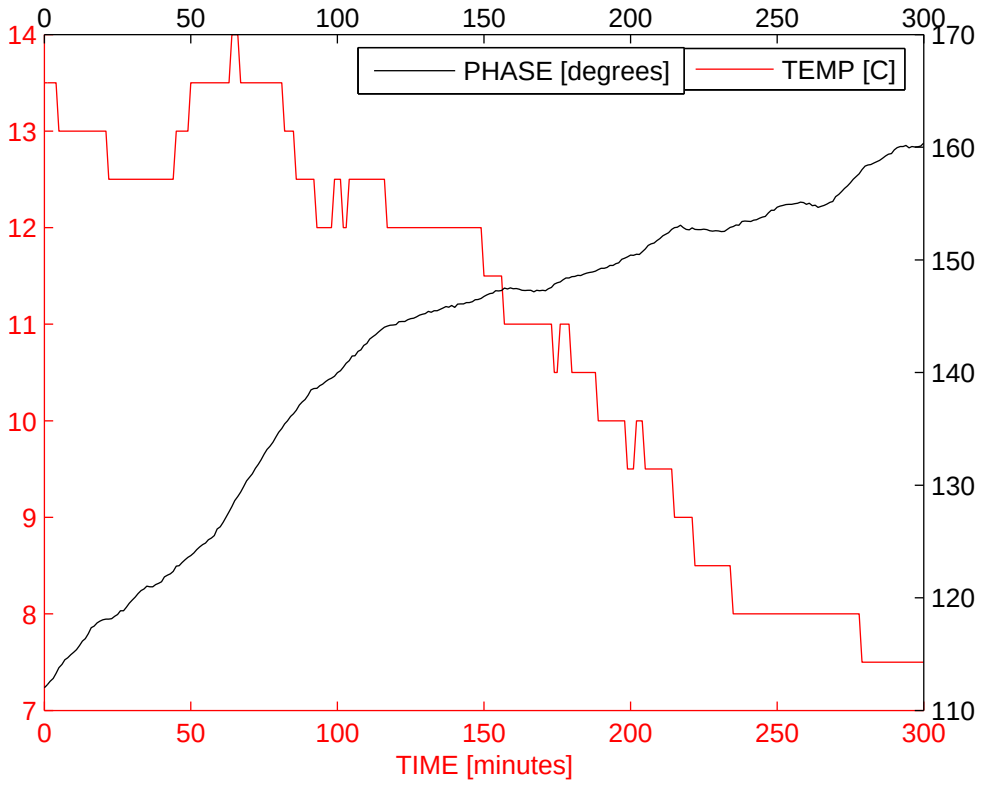

Figure 5.6: Measurements of phase change @ 2 GHz of XDM optical link and temperature during sunset

environment and adds a ± 0.2 degrees[7] uncertainty to the measurement. Temperature is measured with an iButton with an uncertainty of ± 0.5C.

Using this information the uncertainty is calculated as 9 %

5.4.3 Results

The sunset data is shown in Figure 5.6.

5.4.4 Results analysis

As expected we see a linear correlation with a negative slope between the phase and the temperature.

It appears that from minute 150 onwards both the phase and temperature plots have an approximately straight line fit. If we fit straight line models to the phase and temperature plots in this region then the ratio of the gradient of the phase to that of the temperature will be equal to the phase stability with temperature in that region. From 150 minutes onwards the phase gradient is 0.089 degrees/minute and the temperature gradient is -0.030 C/minute. Figure 5.7 shows the temperature and phase plots with the fitted lines.

[7] $\pm\triangle$2C (20 degrees/km/C)(0.004 km)

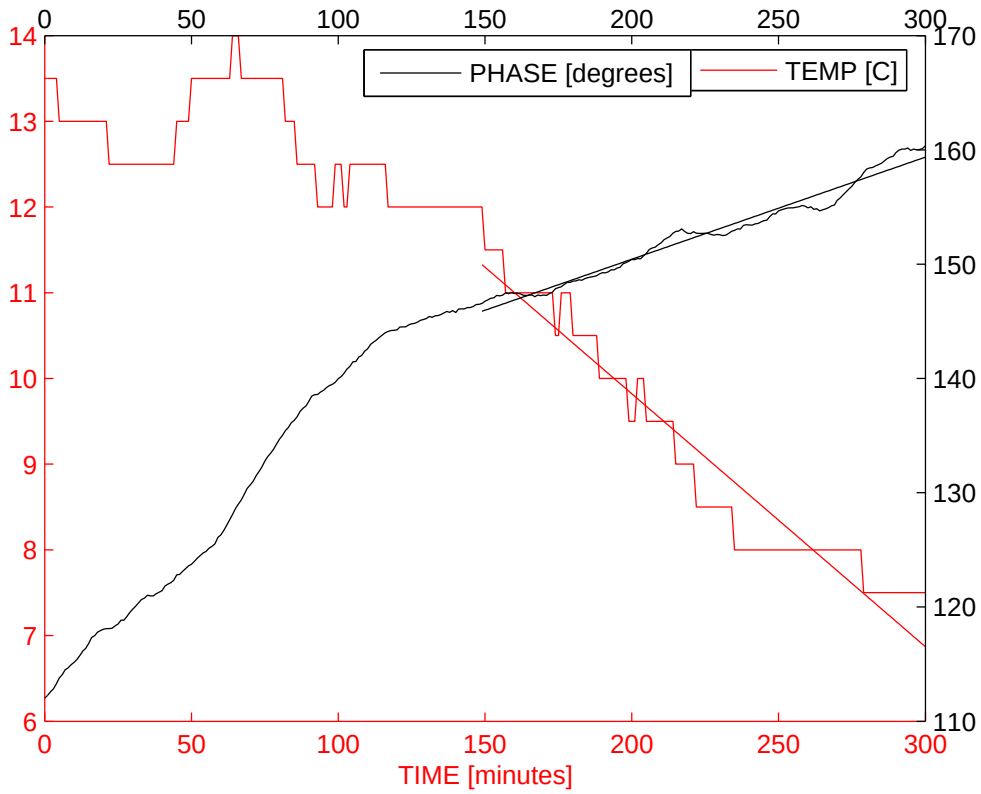

Figure 5.7: Linear regions chosen where the phase and temperature changes linearly with time during sunset to determine the phase stability of the XDM optical link

The phase stability of the link is thus calculated to be -3.0±0.3 degrees/C which results in a phase change of 0.89 degrees over 10 minutes during sunset in the Winter month that the link was measured[8].

5.4.5 Conclusion

The phase stability of the XDM optical fibre installation has been measured during sunset. The link has a phase stability of -3.0±0.3degrees/C which results in a phase change of 0.89 degrees over 10 minutes at sunset during Winter.

5.5 Phase stability during movement of HartRAO dish

The azimuth and elevation movement of the dish causes bending / torsional forces on the optical fibre cable running in the horizontal and vertical cable wraps. This experiments sets out to measure the changes in phase caused by these mechanical stresses on the cable. Appendix B contains a detailed description of the mechanism of the cable wraps used in the XDM dish.

[8] As when calculating the gain stability of the XDM, during Summer the phase change would be higher due to the faster temperature changes

5.5.1 Experiment setup

1. The Photonics transmitter and receiver is connected to the HartRAO link using 2x 2 meter patch cable

2. Experiment starts at around 2 PM when the ambient temperature rate of change is the slowest. This time period was determined from measurements of the preceding 2 days ambient temperature as illustrated in Figure

3. For the azimuth movement measurement, the dish's elevation coordinate is fixed at 90 degrees and the azimuth position is steered to the following positions: [-160 -128, -96, -64, -32 0 , 32, 64, 96, 128, 160] degrees.

4. Readings of the phase @ 2 GHz are measured with a VNA at each azimuth position change of the dish.

5. For the elevation movement measurement, the dish's azimuth coordinate is fixed at 0 degrees and the elevation position of the dish is steered to the following positions: [90, 80, 70, 60, 50, 40, 30, 20, 10] degrees

6. Readings of the phase @ 2 GHz are measured with a VNA at each elevation position change of the dish.

5.5.2 Experimental uncertainty of measurement setup

Each movement run had a duration of a few minutes thus the lab temperature can be assumed to be constant during that time. The temperature component of the VNA uncertainty equation thus falls away and the VNA can be assumed to measure phase with an uncertainty of 0.2 degrees. The phase changes with temperature of the optical fibre link can be assumed to be zero due to the time of day that the experiment takes place and the short duration per movement cycle and thus does not contribute to the uncertainty. The total phase uncertainty of the experiment is thus equal to the VNA uncertainty of ± 0.2 degrees.

The dish position angle has an uncertainty of ± 2degrees. Radio telescopes position angles are generally accurately calibrated as it is required to locate extra-terrestial sources with arc second resolution. This uncertainty however comes about as when entering the desired angle manually the dish position (as displayed on the digital readout[9]) did not move exactly to this desired position (might have been a bug in the dish controller). This offset was also not repeatable between experiment runs and had a spread of about 2 degrees.

[9]The dish position readout is based on a mechanical position encoder in the dish and is the part that is calibrated. One can thus expect this reading to accurately describe the position of the dish.

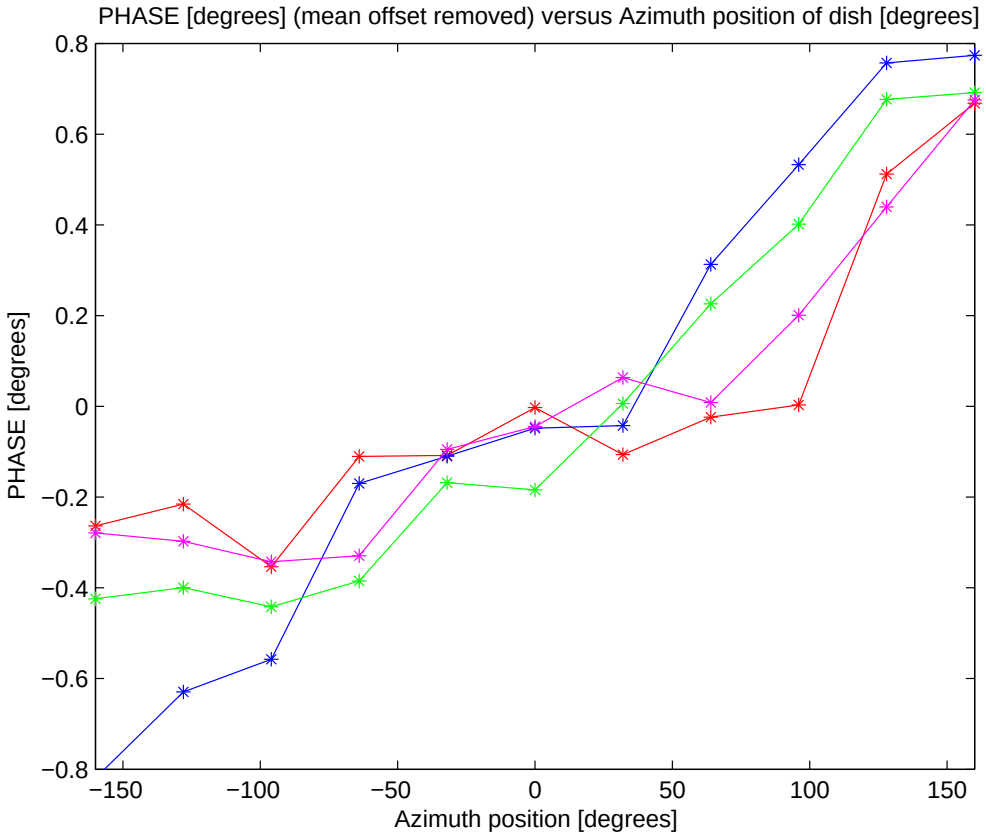

Figure 5.8: RF Phase changes @ 2 GHz of the optical link versus azimuth movement of the XDM dish. Note that the offset of the mean phase has been removed from this graph

5.5.3 Results

The phase versus azimuth position data is shown in Figure 5.8. The phase versus elevation position data is is shown in Figure 5.9.

5.5.4 Results analysis

For the azimuth experiment, the results are repeatable. The phase changes by a maximum of 1.6 degrees over 320 degrees of azimuth movement. From this it appear that the torsional forces on the optical fibre cable, which dominate during azimuth movement, does not have a significant effect on the phase stability

The relationship with elevation movement is less clear, but it seem as though there is an increase in phase with elevation angle. The total phase change is less than 1 degree over 80 degrees of movement.

The worst case phase schange with 10 degrees of azimuth and elevation movement movement is 0.005 and 0.01 degrees respectively

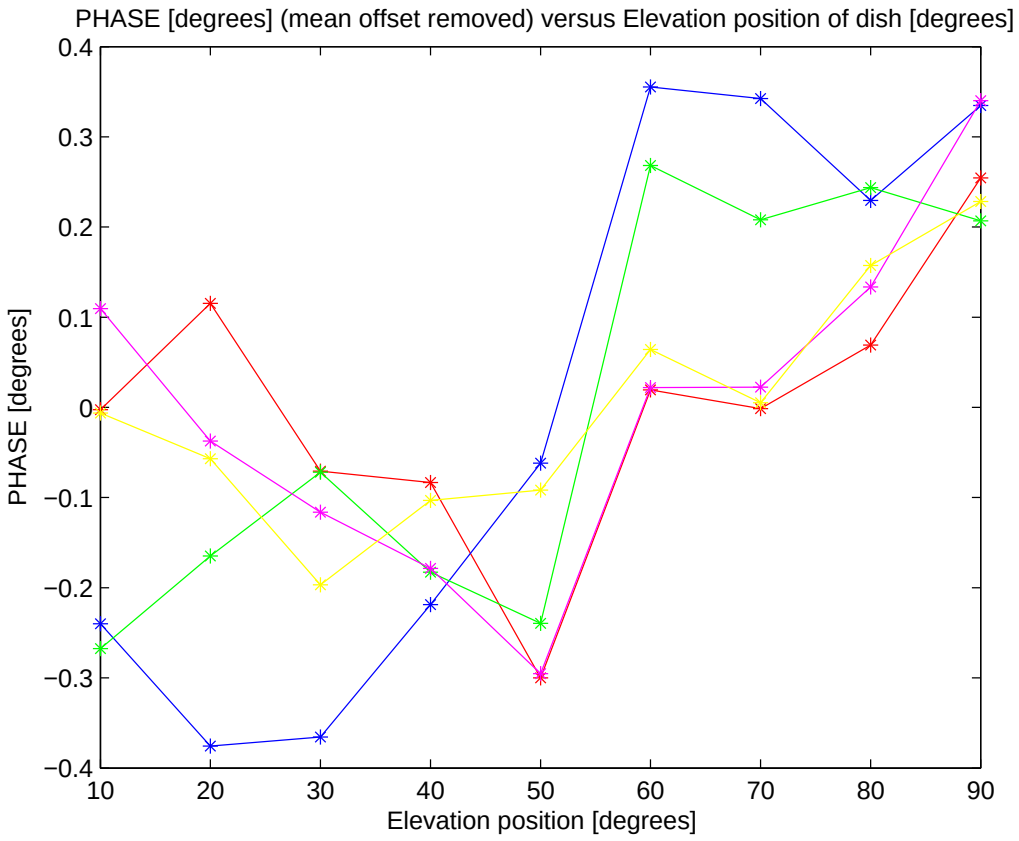

Figure 5.9: RF Phase changes @ 2 GHz of the optical link versus elevation movement of the XDM dish. Note that the offset of the mean phase has been removed in this plot

5.5.5 Conclusion

Phase changes of the optical link due to position changes of the XDM were measured while the dish was moved in azimuth and elevation. The phase results for both azimuth and elevation movement were repeatable between measuring runs. The worst case change with azimuth and elevation movement were 0.005 and 0.01 respectively. From this experiment we see that movement of the dish has practically zero effect[10] on the phase stability of the optical fibre link compared to the thermal effect.

5.6 Conclusion

In this chapter the phase stability of an analogue optical fibre link with temperature was measured. This was done by setting up experiments to measure the phase stabilities of the OTx-ORx and of the optical fibre with temperature. The results of these individual portions of the link were combined in a calculation to check the phase change over 10 minutes (i.e. phase stability) of an analogue optical link inside a thermal environment based on the KAT-7 environment. The phase stability of the analogue optical fibre link is found to be sufficiently stable to pass the KAT-7 apportioned requirements. Further experiments for antenna movement and environmental temperature swings (such as happens during sunset) were performed on the XDM link for additional practical data.

[10] Over 10 degrees of movement as is normally specified

Chapter 6

Dynamic range of optical fibre link

This chapter contains the dynamic range results of measurements made on the Foxcom optical link. As explained in Section 2.3.5 the dynamic range is the ratio of the noise figure to the 1dB compression point.

6.1 Noise Figure

This section describes the measurement of the noise figure of the Foxcom optical link with a short length of fibre[1].

6.1.1 Experiment setup

1. Foxcom link with 2 metre optical fibre patch cable linking the transmitter to the receiver.

2. Agilent NF meter with 6dB ENR Noise head setup to measure NF. Setup is shown in Figure 6.1.

6.1.2 Experimental uncertainty of measurement setup

The Agilent N8973A NF meter, with the Agilent N4000A SNS Noise head with ENR of 6 dB, has an noise figure uncertainty of ± 0.2dB[13].

[1] A better experiment might have been to measure the noise figure with a fibre length representative of the KAT-7 length. A rule of thumb used by Foxcom is that the noise figure increases by 1dB for every extra 1 dB of optical loss by the addition of fibre. Foxcom says that 3 dB of optical loss adds 1 dB to the NF. The 5 km of KAT-7 fibre adds 1.5 dB of RF loss to the system. It generally is easier to improve the noise figure of the link than the 1dB compression point however, so the experiment is sufficient as it stands.

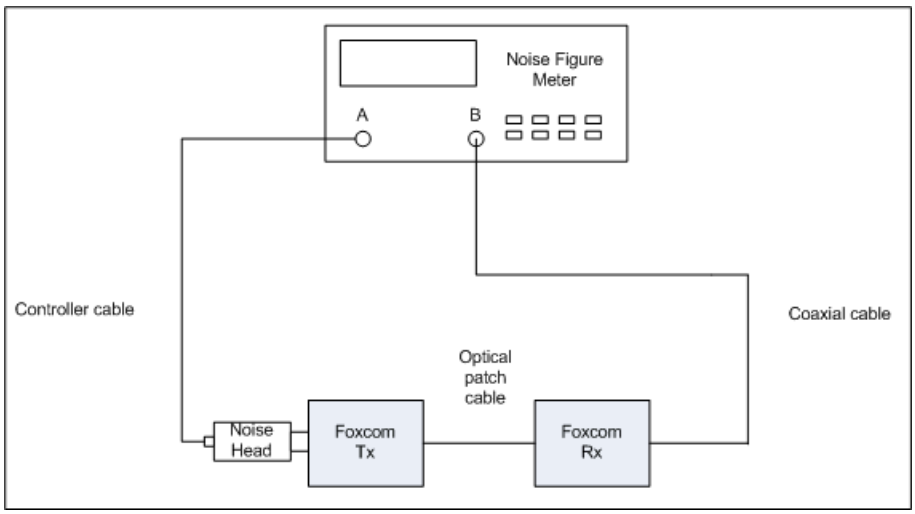

Figure 6.1: Experimental setup to measure the noise figure of the Foxcom RF-over-fibre link

Table 6.1: NF at spot frequencies of the Foxcom optical fibre link (with short fibre) as measured by the NF analyser

Frequency [MHz]	NF [dB]	GAIN [dB]
1000	11.05	19.1
1200	11.74	18.92
1400	12.27	19.05
1600	12.96	18.79
1800	13.51	17.92
2000	13.91	17.9

6.1.3 Results

A table of NF and frequency is shown in Figure 6.1. This table is illustrated graphically in Figure 6.2

6.1.4 Results analysis

The NF of 13.9 dB at 2 GHz (the worst case) is equivalent to a noise temperature $T_n = (F-1)T_0 = (10^{13.81/10}-1)293 = 6752$ K. Inside the KAT-7 bandwidth of 800 MHz this equals a equivalent noise input power of $kT_nB = -71$dBm. For a SNR of 20 dB we should thus choose -50 dBm as the nominal input power into the unit. This represents the lower boundary of the dynamic range requirement. The next section is a measure of the upper bound.

6.2 1% GAIN compression

As explained in Section 2.3.5 the 1% gain compression power level defines the upper level of the dynamic range calculation. The 1% gain compression point equals is 14 dB above

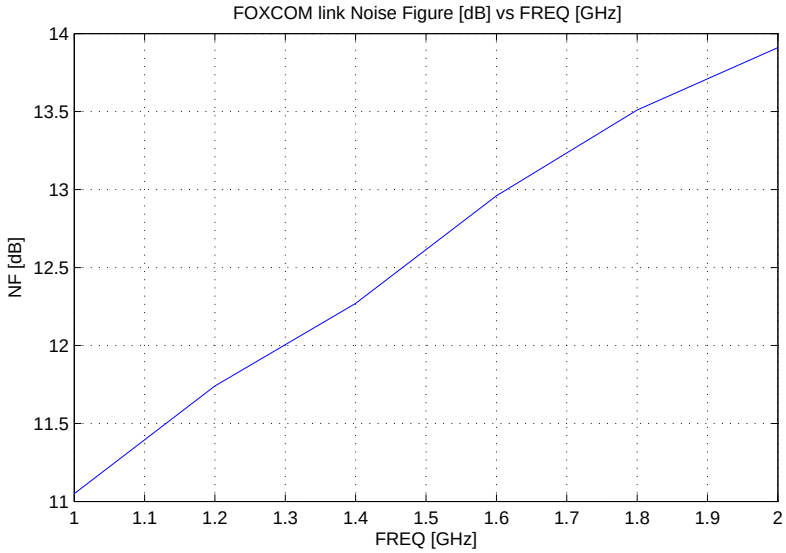

Figure 6.2: Graph of NF vs Frequency of Foxcom optical link (short fibre length). Noise increases linearly (in a log scale) with frequency

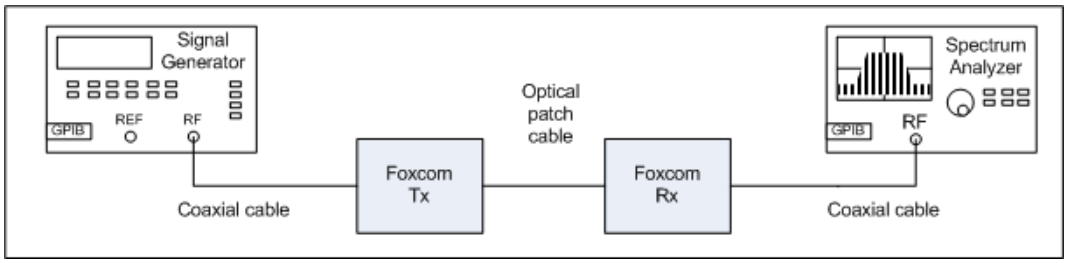

Figure 6.3: 1dB gain compression measurement setup

the 1 dB gain compression. This experiment measure the 1 dB gain compression point.

6.2.1 Experiment setup[2]

1. Foxcom link with 2 metre optical fibre patch cable linking the transmitter to the receiver.

2. A signal generator supplying a 2 GHz CW signal to the optical transmitter at the following powers: Psig_gen = [-30, -25, -20, -18, -15, -14, -13, -12, -11, -10, -9, -8, -7, -6, -5, -4] dBm

3. The spectrum analyser measuring the the output of the optical receiver. The setup is shown in Figure 6.3.

6.2.2 Results

There results are illustrated in Figure 6.4.

[2]In hindsight this experiment setup could be done quicker and more accurately with a VNA

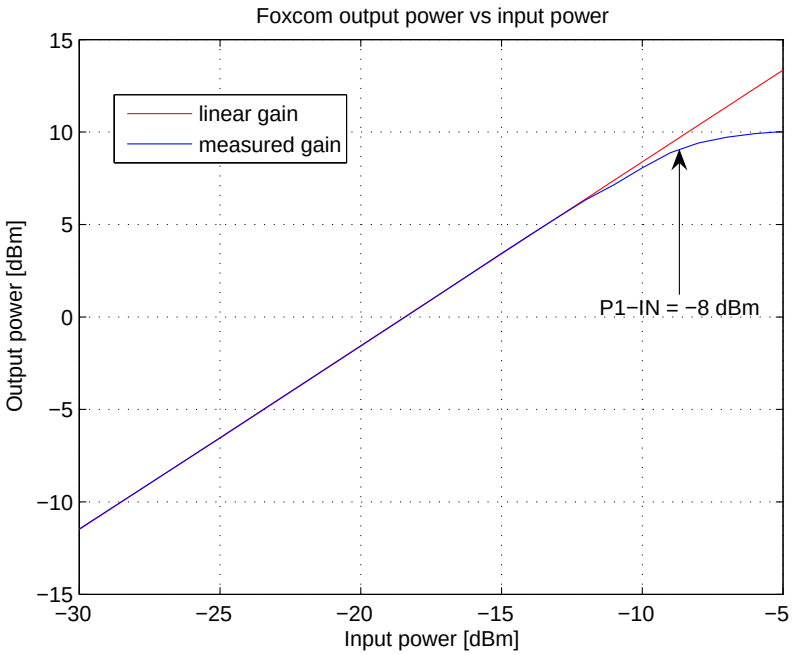

Figure 6.4: Plot of output power versus input power @ 2 GHz of Foxcom RF-over-fibre link showing the linear gain plot, the measured data plot and the input 1dB gain compression power level

6.2.3 Results analysis

Figure 6.4 shows an input 1 dB gain compression of the Foxcom link being -8 dBm @ 2 GHz (worst case). This means that the 1% gain gain compression level is at -22 dBm.

6.3 Dynamic range

Using the definition of dynamic range DR which is the ratio between the 1% gain compression point and the nominal signal level where a 20 dB SNR is achieved, we have DR = -22 dBm -(-50 dBm) = 28 dB. This exceeds the 20 dB headroom requirement as stated in 2.3.5.

6.4 Conclusion

The dynamic range of the Foxcom optical fibre link has been calculated by measuring the noise figure and the 1 % gain compression point. The Foxcom optical link has a headroom of 48 dB which exceeds the KAT-7 dynamic range requirement.

Chapter 7

Conclusions

Radio astronomy places stringent signal fidelity requirements on the RF components and signal transport. In this dissertation an attempt was made to characterise the gain stability, phase stability and dynamic range of analogue optical fibre links and thereby test its suitability for long haul signal transport in the KAT-7 configuration. This chapter draws together the conclusions for each of these performance measures and concludes that analogue optical fibre technology is suitable for the KAT-7 requirements.

7.1 Requirements and performance indicators

The different components of an analogue optical fibre link is stated. Calibration in radio astronomy was introduced and this gives rise to the scan time which is the frequency at which calibration takes place. This is thus the time in which the stability is defined. The important requirements of gain stability, phase stability and dynamic range were introduced, stated and explained. For these requirements the optical fibre link was apportioned a part of the total telescope receiver requirement. The factors influencing these requirements in the optical fibre link were listed and explained. From literature and experiments it was found that temperature, or the thermal environment of the optical fibre link, is the dominant contributor to the gain and phase stability. The thermal environment of the optical fibre link in the KAT-7 system is then defined. This thermal model will be used to check the suitability of the analogue optical fibre link for the requirement of the KAT-7 radio interferometer.

7.2 Tools and methods

In this dissertation a VNA is used to measure the S21 scattering parameter of the optical fibre link under test from which gain and phase is internally calculated and reported by the VNA. The VNA is controlled via an Ethernet link to a PC running Labview software. The Labview software logs the gain and phase. Further processing is done with

Matlab. Temperature is measured throughout the experiment with an iButton temperature logger. For dynamic range measurement, noise is measured with a noise figure meter and gain compression with the combination of a signal generator and spectrum analyser. The XDM telescope is used to make gain and phase measurements during movement and temperature swings of a real optical fibre installation.

7.3 Gain stability

The gain stability of the analogue optical fibre link passes the KAT-7 requirement. From the measurement was found that the temperature changes on the OTx-ORx is the primary contributor to the gain stability of the link. In most cases, the OTx and ORx will be close to the other RF components where cooling is available and thus its environment can be kept sufficiently stable to ensure the necessary gain stability.

7.4 Phase stability

The phase stability of the analogue optical fibre link passes the KAT-7 requirement. It was found that the fibre is the only contributor to the phase stability of the link. Due care needs to be taken in the design of the optical fibre paths to thermally insulate the optical fibre from changing ambient conditions. As seen from the soil thermal model, burying of the optical fibre makes a substantial reduction in the peak to peak temperature variations compared to the top surface of the soil. The susceptible regions of the fibre cable are the transitional areas (going from underground to termination) where there is less thermal shielding. When the optical fibre cable is extended to go the focus of the dish[1], as in XDM, we see that the phase stability requirements can be met[2]. Issues in reliability of the optical cable over the dish's 20 year lifetime then come into play.

7.5 Dynamic range

The dynamic range of the analogue optical fibre link passes the KAT-7 headroom requirement. Note though that the dynamic range has been tested using the headroom definition of 1% compression level less 20 dB above the noise floor. In this dissertation no mention has been made of the RFE requirement of the input power level at which the spurious frequency components are acceptable. Spurious frequency components are essentially in band frequency lines that are generated by the in band frequency components mixing together due to non-linearity's in the system. The $2f_1 - f_2$ and $2f_2 - f_1$components as

[1] In other words, the riser cable becomes an optical fibre cable

[2] at least for the KAT-7 frequencies. Higher frequencies need better group delay stability

explained in Section 2.3.5. The spurious frequencies are characterised by the 3rd order intercept point. More detail can be read in [19].

7.6 Summary of Results

Table 7.1: Summary of the requirements and results of the gain and phase stability and dynamic range measurements in this dissertation

Parameter	Fibre stability factor	OTx-ORx stability factor	Total changes over 10 minutes	Req.	PASS
Gain stability	-0.00045 dB/km/C $\pm$ 0.00003 dB.	-0.019 $\pm$ 0.001 dB/C	0.038 dB	< 0.03 dB	yes (as explained in Section 4.3)
Phase stability	-20 $\pm$1 degrees/km/C	0.1$\pm$0.1 degrees/C	0.26 degrees	< 2 degrees	yes
Dynamic range	n/a	n/a	48 dB	> 40 dB	yes

7.7 Areas of future study

1. A bending jig has been built that models the KAT-7 azimuth cable wrap and subjects any cable to the bending forces for a user-settable amount of cycles. This is important to prove the physical reliability of the optical fibre cable over it lifetime. Further testing is needed to monitor the performance of the candidate optical cables when subjected to repeated bending with this jig.

2. As explained in Section 7.5 more work is need in understand the KAT-7 requirement for dynamic range from the perspective of spurious frequency components. Measurements can also be done using 2 tone measurement techniques.

3. More work can be done on the thermal modelling of the environment of the optical fibre link. Temperature sensors can be distributed throughout the underground section to verify the accuracy of the soil model as well as more precise measurements in the underground to terminal equipment transitional sections.

Appendix A

Labview Code

A.1 Program

Because it is a graphical program it is not possible to fit the program onto this page. It is included on the CD ROM.

A.2 Input parameters

This program has the following input parameters:

1. Which optical input device. This is used as part of the routine to form the filename described in the next section
2. VISA session. This is just used by Labview to find the VNA on the network. I used the following input: RSIB::192.168.20.135::INSTR, where the IP address is that of the VNA
3. Measurement interval in minutes
4. Number of intervals. Thus minutes andnumber of intervals defines the duration of the experiment

A.3 Output parameters

The program has the following outputs:

1. BUSY logging indicator
2. Current interval
3. The 3 data files containing the S21 values of GAIN, GROUP DELAY and PHASE
4. Error window. The error message is contained there if there are any errors

A.4 Filename format

The format of the filenames of the 3 files is DDMMYY_HHhMM_DeviceMeasuredparameter.txt, where:

DDMMYY_HHhMM is the start date and time of the experiment

Device is the device selected as described in the Input parameters section above

Measuredparameter is one of S21_dB, S21_group_delay or S21_phase which distinguishes the 3 files from one another.

Example: A file with the name '280708_15h45_PhotonicsS21GAIN.txt' would contain data measuring the S21 (i.e. GAIN) in dB of the Photonics Optical link on the 28th July 2008 starting at 15h45

A.5 File format

Each of the files are structured as follows:

The first row contains the frequency vector

The 2nd row and each subsequent row contains the formatted measured data vector. Thus position (2,1) would be the data at freq_start and (2,2) would be the 2nd point corresponding to (freq_start + delta_f), etc. Data (3,1), would be the point corresponding to freq_start of the 2nd data vector.

A.6 Other information

The program assumes that 3 channels that have been calibrated exist. It uses the currently set number of points, Pout, averaging, freq_start and freq_stop settings[1].

[1]It has been found that the implementation described above is a slow method of collecting data and proves problematic when needing a faster sampling time for example during dynamic measurements. Newer versions of this software exist that for example uses 3 traces of the same calibrated channel. This speeds things up tremendously. Contact the author of this dissertation for further information.

Appendix B

Mechanical detail of cable wrap

This section describes the azimuth and elevation cable wraps on the XDM dish

B.1 Elevation Cable Wrap

Figure B.1 shows the elevation cable wrap. It is apparent from the photo that the cable is routed inside this wrap and the cable is mostly subjected to bending forces. If one stands facing the dish in the perspective of the person that takes the photo, the the top side of the dish will move away from you as it decreases in elevation angle. Figure B.2 shows another picture of the XDM dish with the elevation at a lower angle, notice the shape of the azimuth cable wrap. It is clear that the amount of bending increases as the elevation angle of the dish is decreased. .

B.2 Azimuth cable wrap

Starting with a thought experiment: if one has a pencil attached to a fixed platform on the bottom end. Above the pencil and not touching one has a rotating platform. If one now attaches a string to the moving platform above and the fixed platform below, then as the moving platform above rotates, the string will twist around the pencil. This is the principle of the XDM azimuth cable wrap. Now instead of a string, a metallic chain is attached to the fixed platform below and rotating platform above. At 3 locations through the length of the cylindrical pipe (representing the pencil), a freely moving concentric circular metal bracket is attached to the chain to facilitate the wrapping of the chain around the cylindrical pipe. The various riser cables are attached to this bracket. Figure B.3 shows the azimuth cable wrap in the rest position (at about -40 degrees) . Figure B.4 shows the azimuth cable wrap at the extreme clockwise angle (representing an angle of around 230 degrees. Note the torsional wrapping of the cables around the cylindrical pipe . A ‘twisting bias’ exist on the XDM riser cable. Perhaps because the antenna is left in

Figure B.1: Image of elevation cable wrap at 90 degrees of elevation

a particular position most of the time, thus on the anti-clockwise extreme, the cables are not twisted as much as in the clockwise extreme as illustrated in the picture.

Figure B.2: Elevation cable wrap at a lower angle. The cable wrap at this lower dish angle position subjects the riser cable to more bending

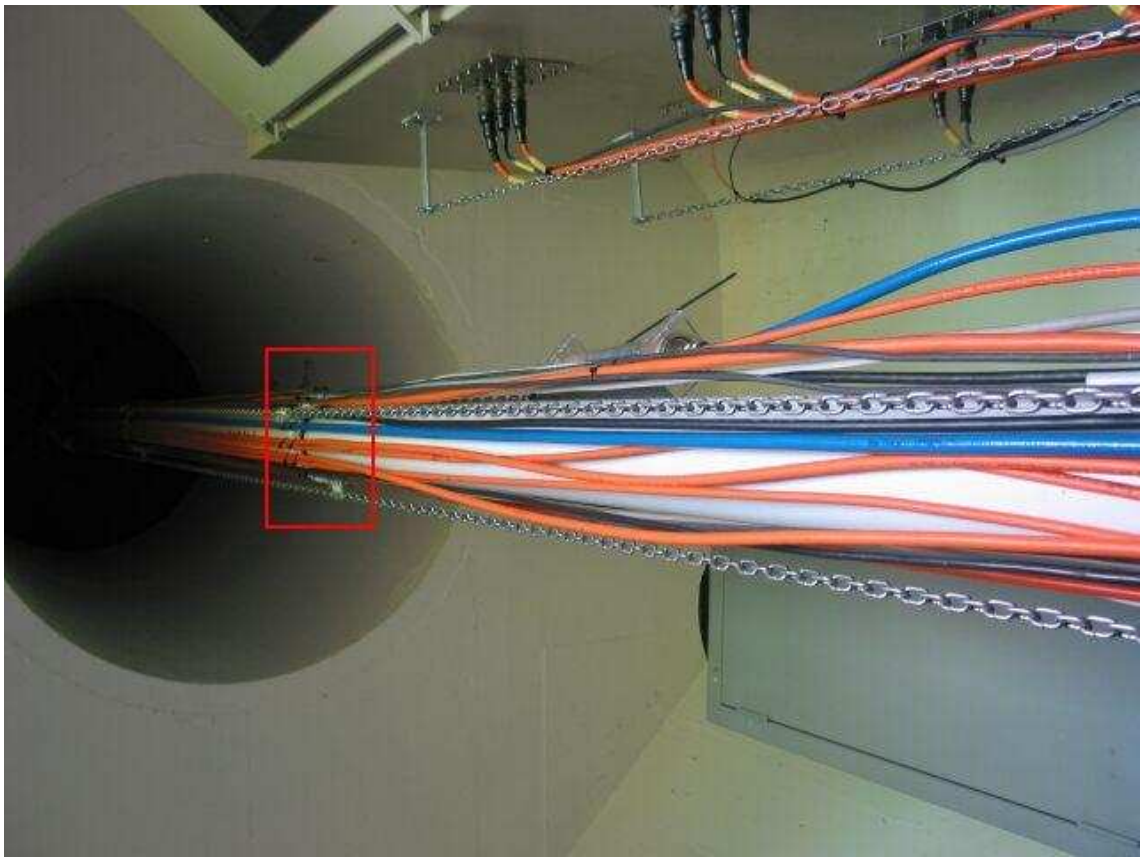

Figure B.3: XDM Azimuth cable wrap at rest position. Notice the wrapping chain (the red block), the rotating bracket, the cylindrical pipe and the various riser cables

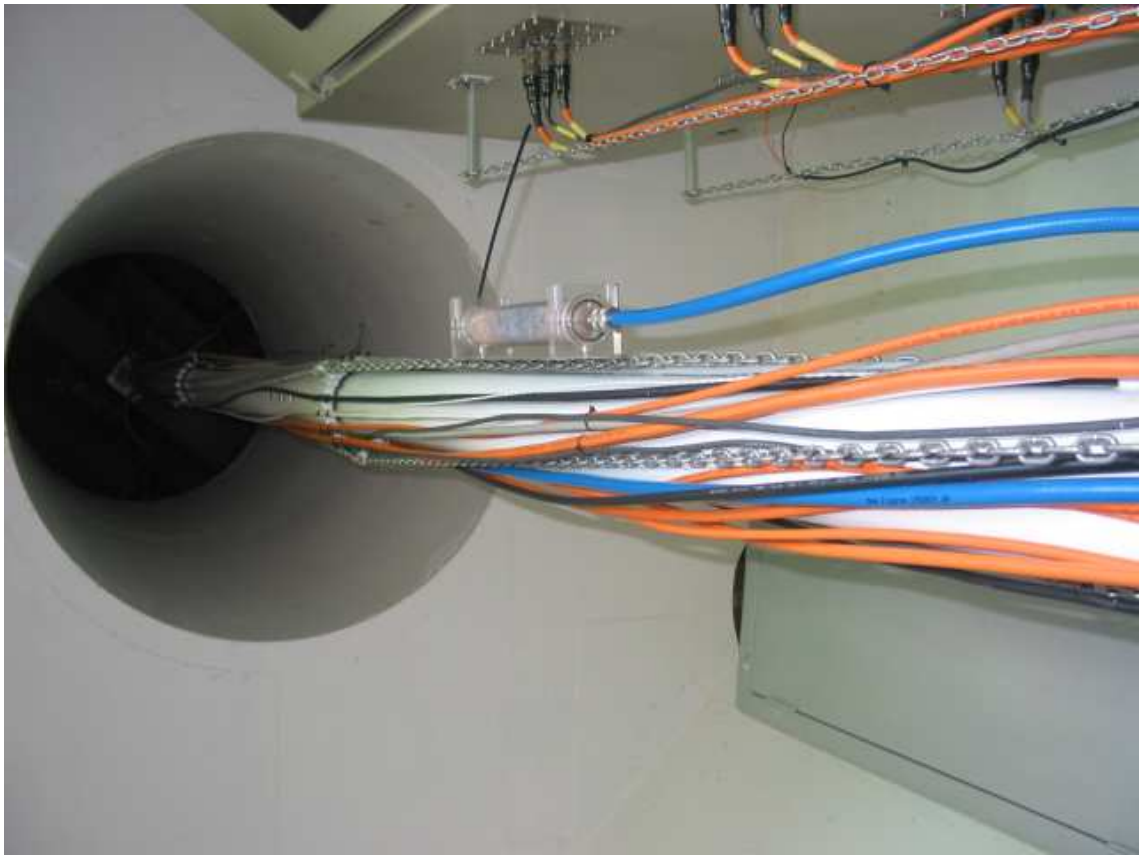

Figure B.4: XDM azimuth cable at the extreme clockwise direction. This represents an azimuth angle of around 230 degrees. Notice the wrapping/twisting around the cylindrical pipe.

Bibliography

[1] Agilent. Fundamentals of rf and microwave noise figure measurements an 57-1. Technical report, Agilent, 2006.

[2] Astron. How does a radio telescope work. http://www.astron.nl/about-astron/press-public/what-radio-astronomy/how-does-radio-telescope-work/how-does-radio-telescop, 2009.

[3] J. Carr, S. Saikkonen, and D. Williams. Single mode optical fiber index of refraction dependance on product parameters, tensile stress and temperature. Technical report, Corning Incorporated, 1990.

[4] Corning. Corning leaf optical fibre, 2008.

[5] C. Cox. *Analog Optical Links - theory and practice*. Cambridge University press, 1 edition, 2004.

[6] L. D'Addario. Memo 466: Gain stability: Requirements and design consideration. Technical report, ALMA, May 2003.

[7] G.Lutes and W.Diener. Thermal coefficient of delay for various coaxial and fiber-optic cables. Technical report, JPL Communications Systems Research Section, 1989.

[8] Google. Google earth image of xdm. www, 2009.

[9] J. Kraus and A. Moffet. *Radio Astronomy*, volume 35. AAPT, 1967.

[10] S. Kumar. Rf over fiber - current trends. Presentation.

[11] T. Kusel. *KAT-7 Telescope Requirement Specification*. MeerKAT project, 1.1 edition, Dec 2008.

[12] M. Levine. Memo 97 modified azimuth cable wrap. Technical report, Submillimeter Array, 1996.

[13] A. Mngadi. Noise figure analyser decision. Technical report, Square Kilometre Array South Africa, 2007.

[14] R. Nelson. What are s-parameters, anyway? *Test & Measurement world*, Jan 2001.

[15] NRAO. How radio telescopes work. http://www.nrao.edu/index.php/learn/radioastronomy/radiotelesc 2007.

[16] A. Peens-Hough. *KAT-7 Signal path Architecture*. MeerKAT, 0.e edition, 10 2008.

[17] A. Peens-Hough. Private communication, 2008.

[18] Perley and Hayward. Evla memo 110: The effect of amplifier compression by narrow band rfi on radio interferometric imaging. Technical report, NRAO, 2007.

[19] D. Pozar. *Microwave and RF Design of Wireless Systems*. Wiley, 2000.

[20] R.McCool. Enhancing the sensitivity of radio telescope using fiber-optic networks. Technical report, URSI, 2006 2006.

[21] Rohde&Schwarz. Remote control of r&s spectrum and network analyzers via lan. June 2003.

[22] S. SA. South afirca's bid to host the ska. http://www.ska.ac.za/bid/index.php, 2008.

[23] J. Sarkissian. On eagle's wings: The parkes observatory's support of the apollo 11 mission. In *Publications of the Astronomical Society of Australia*, volume 18. Astronomical Society of Australia, 2001.

[24] S.Durand and T.Cotter. Operational performance of the evla lo round-trip phase system. *EVLA Memo*, 44, 2002.

[25] J. M. Senior. *Optical Fiber Communications*. Prentice Hall, 2 edition, 2005.

[26] Test and M. division. *Operating manual*. Rohde&Schwarz, 1.9 edition, 2008.

[27] A. Tiplady. Phase stability in fibre optic cables for meerkat. Technical report, SKA SA, March 2009.

[28] T.Kusel. *KAT-7 RF Front end Specification*. Karoo Array Telescope, 2 edition, 2009.

[29] Wikipedia. Labview - wikipedia, the free encyclopedia. http://en.wikipedia.org/wiki/Labview, Nov. 2008.

[30] Wikipedia. Matlab - wikipedia, the free encyclopedia. http://en.wikipedia.org/wiki/Matlab, Nov. 2008.

[31] Wikipedia. Radio astronomy - wikipedia, the free encyclopedia, Nov. 2008.